

**POSITION CONTROL OF LASER BEAM FOR
FREE SPACE OPTICS COMMUNICATION**

BY

SYED AHSAN MASUD ZAIDI

**A Thesis Presented to the
DEANSHIP OF GRADUATE STUDIES**

KING FAHD UNIVERSITY OF PETROLEUM & MINERALS

DHAHRAN, SAUDI ARABIA

**In Partial Fulfillment of the
Requirements for the Degree of**

MASTER OF SCIENCE

In

ELECTRICAL ENGINEERING

MARCH 2019

KING FAHD UNIVERSITY OF PETROLEUM & MINERALS
DHAHRAN 31261, SAUDI ARABIA

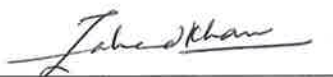
DEANSHIP OF GRADUATE STUDIES

This thesis, written by **SYED AHSAN MASUD ZAIDI** under the direction of his thesis adviser and approved by his thesis committee, has been presented to and accepted by the Dean of Graduate Studies, in partial fulfillment of the requirements for the degree of **MASTER OF SCIENCE IN ELECTRICAL ENGINEERING DEPARTMENT**.

Thesis Committee



Dr. Salim Ibrir (Adviser)



Dr. Mohammed Zahed Mustafa Khan
(Member)



Dr. Alaa El-Din Hussein (Member)



Dr. Abdallah Al-Ahmari
Department Chairman



Dr. Salam A. Zummo
Dean of Graduate Studies

23/4/19

Date



©Syed Ahsan Masud Zaidi
2019

*This work is possible due to the support of the my family , fiends
and colleagues.Specially I would like to dedicate this work to my
beloved father Syed Khurshid Ali Zaidi.*

ACKNOWLEDGMENTS

I would like to express my gratitude to King Fahd University of Petroleum and Minerals for supporting this work.

I would also like to thank Professor. Salim Ibrir Dr. Zahed Mustafa Khan and Dr. Alaa El-Din Hussein for their support and guidance as my advisors.

TABLE OF CONTENTS

ACKNOWLEDGEMENT	v
LIST OF TABLES	viii
LIST OF FIGURES	ix
LIST OF ABBREVIATIONS	xii
ABSTRACT (ENGLISH)	xiii
ABSTRACT (ARABIC)	xiv
CHAPTER 1 LITERATURE SURVEY	1
1.1 Introduction	1
1.1.1 Actuation Mechanisms	5
1.1.2 Sensor	12
1.2 Controller Design	14
1.3 Proposed Control Method	23
1.4 Thesis Organization	24
CHAPTER 2 EXPERIMENT LAYOUT	25
2.1 Helium-Neon Laser	29
2.2 Position Sensor	31
2.3 K-Cube Position Sensing Detector (PSD) Auto Aligner .	32
2.3.1 PINs Overview for Auto Aligner	34

2.4	Mirror Actuator	36
2.5	Open Loop Piezo Controller MDT694B	37
2.6	Beam Splitter	38
CHAPTER 3 LASER BEAM SPOT TRACKING USING IMAGE		
	PROCESSING TECHNIQUES	41
3.1	Motivation	41
3.2	Experimental Setup	43
3.3	Color Detection	45
CHAPTER 4 FEEDBACK CONTROL OF PIEZO ELECTRIC		
	STICK-SLIP ACTUATOR	53
4.1	Introduction	53
4.2	Working principle	56
4.3	Input Voltage Dynamics	59
4.4	General Control Scheme for Stick Slip Actuators	61
4.5	Experimental Results: Proportional Control	63
4.6	Proportional Integral Control	67
4.7	System Identification	69
CHAPTER 5 CONCLUSION AND FUTURE WORKS		73
APPENDIX A EQUIPMENT LIST		76
APPENDIX B PSD PIN DIAGRAM		77
APPENDIX C DATE SHEETS		78
	Bibliography	90
	VITAE	100

LIST OF TABLES

Table 2.1	Typical HeNe Parameters	30
Table A.1	Main parts used in the experiment.....	76
Table B.1	Pin Diagram of PDQ80A Position Sensor	77

LIST OF FIGURES

Figure 1.1.	General Free Space Optics experimental setup	3
Figure 1.2.	Servo motors used to steer the laser beam [1]	7
Figure 1.3.	Stick Slip Actuator construction used in [2]	11
Figure 1.4.	Receiver photodiodes arrangement [3] [1].....	13
Figure 1.5.	A Typical Charged Coupled Device (CCD) sensor	13
Figure 1.6.	A Photo Sensitive Detector.....	14
Figure 1.7.	Schematic laser jitter control of test bed used by [4].....	17
Figure 1.8.	Hybrid Control for FSM [5]	17
Figure 1.9.	Optical path schematic used in [6].....	18
Figure 1.10.	optical path used in [6].....	19
Figure 1.11.	Exploded view of FSM in [7]	20
Figure 1.12.	precise model of PSFM [8]	20
Figure 2.1.	Experimental Setup.....	25
Figure 2.2.	Color Detection Setup.....	27
Figure 2.3.	Complete Experimental Setup	28
Figure 2.4.	HeNe Laser beam	29
Figure 2.5.	Optical Resonator Cavity	29
Figure 2.6.	PDQ80A sensor placement	31
Figure 2.7.	KPA101 Auto Aligner.....	33
Figure 2.8.	Connections on Front and rear panel of KPA101.....	34
Figure 2.9.	3-axis Piezo actuator (front and back view).....	36
Figure 2.10.	Open-loop Piezo Controller.....	37

Figure 4.16. System identification Labview Block Diagram	72
--	----

LIST OF ABBREVIATIONS

FSM	Fast Steering Mirror
FSO	Free Space Optics
ILC	Iterative Learning Control
P	Proportional
PI	Proportional Integral
PID	Proportional Integral Derivative
PSD	Photo Sensitive Detector
SSPA	Stick Slip Piezo Actuator

THESIS ABSTRACT

NAME: Syed Ahsan Masud Zaidi

TITLE OF STUDY: Position Control of Laser Beam for Free Space Optics
Communication

MAJOR FIELD: Electrical Engineering Department

DATE OF DEGREE: March 2019

In Free Space Optics(FSO) system light propagation is used to transfer data wirelessly. Due to longer travel distances the precise and accurate tracking of the laser beam becomes a crucial problem. The goal of this study is to develop a laser control system which can precisely track the position of laser beam and reject any minute external disturbances such that a reliable optical connection between laser transmitter and receiver is established. To control the beam position a very sensitive actuator is needed which can move the laser beam in the order of μ meter/ degree .A vision based laser beam spot sensing mechanism was devised to accurately measure the beam spot position.In this study A Piezo actuated stick slip based linear actuator is controlled by a close loop feedback P and PI control to achieve the position accuracy of 3.5 and 0.2 μ meter respectively.

ملخص الرسالة

الاسم:

سيد احسن مسعود زيدي

عنوان الدراسة:

التحكم في توجيه شعاع الليزر للاتصال البصري المباشر

التخصص:

قسم الهندسة الكهربائية

تاريخ الدرجة العلمية: رجب ، 1440

في نظام FSO، يتم استخدام إنتشار الضوء لنقل البيانات لاسلكيًا. نظرًا لطول مسافات الاتصال، يصبح التتبع الدقيق لحزمة الليزر مشكلة حرجية. الهدف من هذه الدراسة هو تطوير نظام تحكم بالليزر يمكنه تتبع موقع شعاع الليزر بدقة والتغلب على أي اضطرابات خارجية دقيقة من أجل تأسيس اتصال بصري موثوق بين جهاز إرسال واستقبال الليزر. للتحكم في موضع الشعاع ، هناك حاجة إلى مشغل حساس للغاية يمكنه تحريك شعاع الليزر بدقة جزء من المليون للمتر لكل درجة. تم تصميم آلية لاستشعار بقعة شعاع الليزر تستند إلى الرؤية لقياس موضع الحزمة الضوئية بدقة. في هذه الدراسة يتم التحكم في المشغل الخطي القائم على الانزلاق بواسطة تحكم نظام مغلق بخوارزيم من نوع طردي (P) و طردي تكاملي (PI) لتحقيق دقة موضع تبلغ 3.5 و 0.2 جزء من المليون من المتر على التوالي

CHAPTER 1

LITERATURE SURVEY

1.1 Introduction

Improving communication is one of the key problems the scientific research is focused on. Starting from the first telephone device made by Alexander Graham Bell in 1876 and the radio communication made by Guglielmo Marconi in 1895 in Italy, communication is improved by a large amount. Current most widely accepted modes of communication is by using fiber optics, or through Wide Local Area Network (WLAN). Although these methods provide a fast and reliable communication there is always room for improvements. Fiber optics provides good data transfer rates but the setup costs for fiber optics are high. WLAN is also a convenient option but since we are not sending the data to a single user WLAN have a risk of signal interception and power losses.

Fiber optics provides good data transfer rates but the setup costs for fiber

optics are high. Wide Local Area Network (WLAN) is also a convenient option but since we are not sending the data to a single user WLAN have a risk of signal interception and power losses. Free space optical system(FSO) is a relatively new communication system which uses a collimated beam of the visible spectrum (e.g laser) to send and receive data [8–11]. According to [12] a data transmission rate of 10Gbps can be achieved from the FSO system. Free space optical system (FSO) find its applications in many areas including cellular phones, televisions, radios, wireless remote, many communication protocols (Wifi, Zigbee, etc), smart cars, many biomedical devices and satellites, etc [13]. Free space optical system is useful for fast and secure data transmission. A data transfer rate of 0.5 Gbps was achieved for a free space optics (FSO) system by S.Muta et al [1]. While the maximum data transfer rate which we can achieve is 2.5 Gigabytes per second [14]. However, the problem in FSO systems is that it requires a very precise control of the laser beam so that the data is not lost with external conditions altering the path of laser.

In our experiment we want to develop a free space optical system (FSO) using a visible light collimated laser beam. The scope of this study is focused mostly on the control of the laser beam spot such that a it is able to reject external disturbances. A camera-based color detection algorithm is developed to sense the laser beam position.we will use either a mirror actuator to divert the beam towards the laser receiver or we will use motorized stages to move the laser itself such that

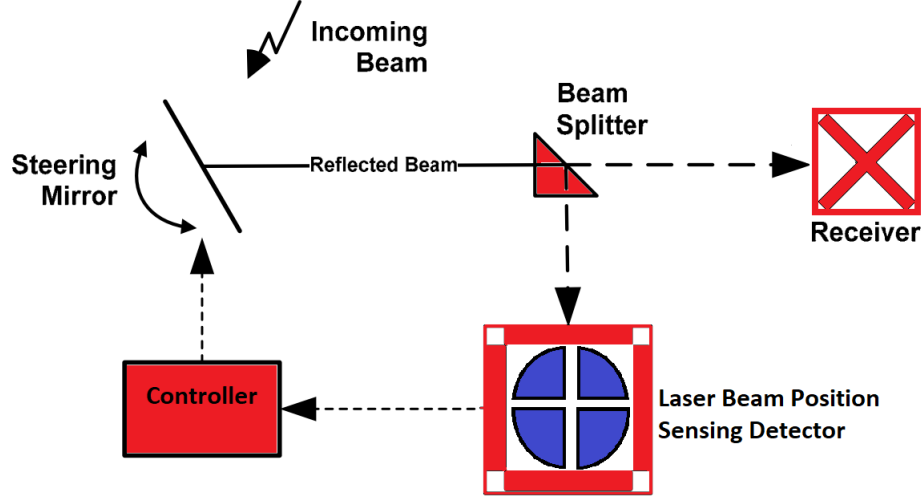


Figure 1.1: General Free Space Optics experimental setup

the laser beam is pointed accurately towards the receiver. We will apply a control algorithms like proportional Integral Derivative (PID) control or Iterative learning control (ILC) to precisely control the position of the beam.

Figure 1.1 shows an example of such a system. A Free space optics (FSO) system works just like a fiber optics transmission system. The difference is that instead of using optical fiber, free space is used as a carrier medium and a collimated laser beam is passed through the air. In FSO systems we can transmit the signal to the range of several kilometers. However, the large transmitting distances require perfect atmospheric conditions like clean air, uniform atmospheric pressure, temperature e.t.c. [12] When a Laser beam is transmitted in free space, very small perturbation at the transmission end could cause a very large offset of the beam at the receiver end. Thus a need for a precise and fast control system arises which can reject the disturbances efficiently and maintain a reliable and automated connection between laser beam transmitter and receiver.

The beam could be stabilized by various methods and a continuous feed of data could be obtained at the receiver end. FSO gives us promising results however many external factors like absorption, turbulence, scattering, and extreme weather conditions made it difficult to achieve the desired results from FSO [15] [14] [16]. A Free space optical system for a laser beam of 1310/ 1550 nm wavelength was designed and laser beam tracking was discussed in [17]. Four degrees of freedom motorized actuator was used for beam steering. They also used a photosensitive detector (PSD) and collimators to complete their FSO experiment. They received the power of -16dbm and found out that in their design the bit rate error is always less than 10^{-11} .

Several types of FSO experiments were discussed in literature. [1,3,5,11,18].A Free space optics communication could mainly be divided into following sections.

- Communication
- Actuation
- Position Measurement
- Control

Since our main focus is on the control of the laser beam, we will discuss about the actuation mechanisms, laser beam spot position measurement and the control schemes, laser beam position measuring and the control algorithms.

1.1.1 Actuation Mechanisms

Several actuator types were used for laser beam steering and control. we can divide some of the available actuators that can be effectively used to steer the laser beam into following categories

Motorized mechanism: A servo motor or a simple dc motor could be used to rotate a mirror. The rotation of mirror could be used to steer the laser beam.

Tip tilt actuator: This is the most common type of actuators that are used for steering the laser beam. A Piezoelectric or mems based material is used to rotate a mirror which is used to steer the laser beam.

Stick Slip Actuators: These type of actuators are an extension of piezo actuators. They provides better dynamic range as compared to a simple piezoactuator. They can be used in linear and tip tilt scheme.

In the following sections we will now discuss some brief applications on these types of actuators used in literature.

Motorized mechanisms

Motorized mirror mount provides the simplest solution among all. Motors have simple constructions, cheap cost, and easy availability. In motorized mechanisms

movement range is not a big problem. The actuator can rotate from 0-360 degrees easily. Due to the absence of piezoelectric materials motorized mechanism generally, don't have the problem of nonlinearities like creep and hysteresis [19]. However, the accuracy provided by the motorized mechanism is not as good as compared to the other devices. In [1, 3], the authors have developed an opto-mechatronics system to control the beam and to reject external disturbances. Two mirrors mounted on servo motors were used at the transmission end to direct the beam towards the receiving photodiode. They used 4 diodes surrounding the main receiving photodiode to detect the position of the laser as shown in Fig 1.2. S.Muta [1] used a proportional control of servo motors to direct the beam towards the receiver.

In [20] the authors have used two sets of servo motors, to steer the laser beam towards the desired location. Authors have discussed the servo motors design and implementation for a laser tracking measurement system. They were able to successfully track the laser beam with accuracy in terms of $500\mu m$ of dynamic error. In [21] the authors have used a quanser's experimental setup for laser beam stabilization. The experiment uses a voice coil and a dc motor to steer the laser beam. By using a sliding mode control the authors have stabilized the beam, however, the movement accuracy is again in the order of millimeters.

A lightweight, portable free-space optical system was discussed in [22], This system could be mounted on mobile platforms and it is able to perform optical communication with a range of at least 50 m. The authors use two servo motors

to steer the laser beam in two dimensions. Quanser has developed a laser beam stabilization experiment [23]. In [21, 24] a fractional order control was developed and discussed on the same quanser laser beam stabilization experiment. The positioning error was in the order of millimeters. In [25] an iterative control scheme was implemented on a motorized beam steering mirror. The resultant was able to track the laser beam with the accuracy of 1 micrometer.

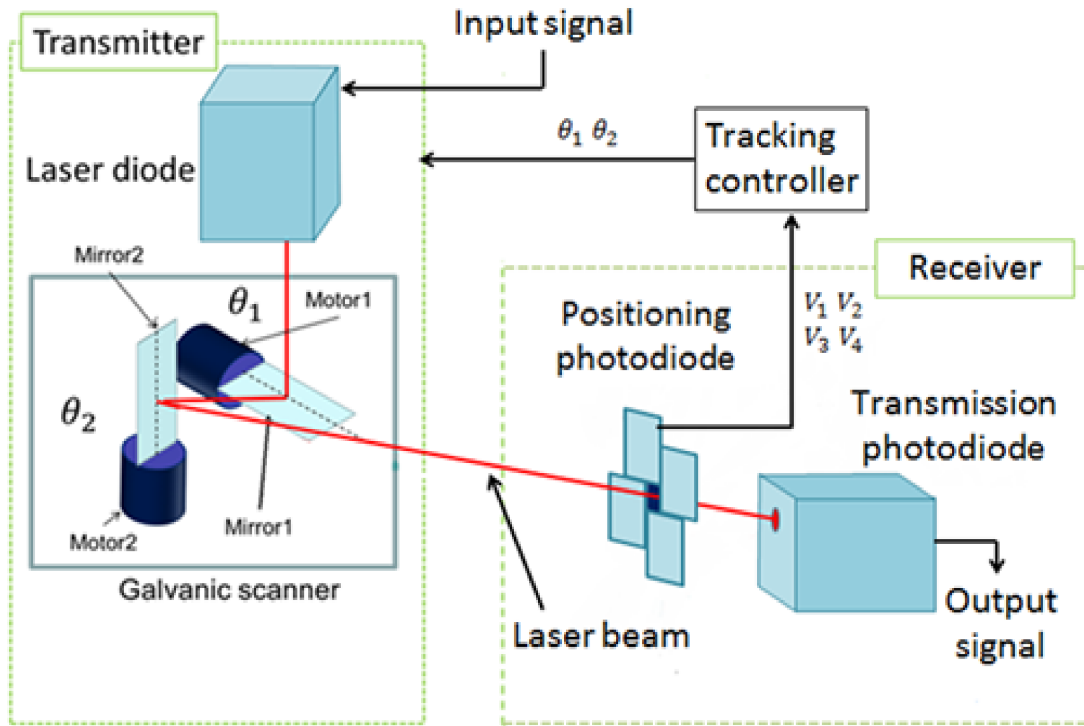


Figure 1.2: Servo motors used to steer the laser beam [1]

Tip Tilt Actuators

Tip-tilt actuators are among one of the most common type of actuators that are used for laser beam steering applications. In optics 'tilt' corresponds to the

deviation of the laser beam direction. Thus a tip-tilt actuator corrects the laser beam direction by rapidly changing its angle in two dimensions. Several types of tip tilt actuary are proposed in literature including Micro Electro Mechanical Systems(MEMS) type , deformable mirror types and piezoelectric tip tilt mirrors. In [11] a laser beam control system including piezo driven mirrors and four quadrant laser beam detector was presented for a micro positioning application. In [26] a micro opto electro mechanical system (MOEMS) type tip tilt mirror is proposed. The proposed mirror has an angular range of ± 4 degrees. In [5] the authors presented the modeling and control for a piezoelectric based mirror mount and by performing a model based hybrid control, they were able to control the laser beam with an error of 0.008mrad. In [27] tip tilt mirror is used to control the laser beam position. The positioning accuracy for this kind of setup was around 0.004m.

In [4] a laser beam jitter control technique was implemented on a fast steering mirror (FSM). The proposed algorithm was able to reject the disturbances with the accuracy in order of micro meters. Perez [6] developed an observer based intensity feedback control for the application on laser beam tracking. They used a microelectromechanical (MEMS) based fast steering mirror. By using an observer based control scheme they were able to track the laser beam with an error of the order of millimeters. In [7] a new two dimensional FSM model is discussed. The authors have proposed a compensation algorithm to reduce the inherent nonlinearities present in piezoelectric actuators. The resultant actuator

has a scanning range of 2 degrees with less nonlinearities.

Piezo actuators are one of the most widely used actuators in the field of micro and nanopositioning applications. Piezo actuators provide excellent movement accuracy. However, the movement range of piezo actuators are very limited. Piezoelectric actuators also have nonlinear behaviors like creep and hysteresis [19]. Creep is a behavior observed in piezoelectric materials which occurs due to the slower realignment of the crystalline domains in the field applied. Due to creep the piezoelectric material keeps on moving even when the applied voltage is dropped.

We can see creep as an inertial effect which keeps moving the actuators even when there is no input. Another typical nonlinearity associated with piezo actuators is the hysteresis effect. Due to this behavior, the position of the piezoelectric material does not depend only on the voltage amplitude applied but rather than the previous values. In simpler words, the position associated with a specific voltage in moving forward is not the same when moving backward. Although piezoelectric materials do have some inherited nonlinear effects the excellent movement accuracy made them a suitable candidate to be used in Free Space optics application.

In [28], authors have proposed another dynamic mirror actuator for laser beam tracking problem. The authors have proposed a low order liner plant model for a piezo-actuated mirror. In [29] the authors presented a three degree of freedom (DOF) piezo-actuated mirror model for laser beam steering and control

application. The proposed model successfully calculates the hysteresis and the dynamical model of the mechanism. A microelectromechanical system (MEMS) based mirror was developed in [30]. The mems based mirror was able to track the reference with the accuracy in millimeters. A control scheme for a Tip tilt mirror was also discussed for adaptive optics in [31]

Stick Slip Actuators

These types of actuators provides promising results for free space optics systems control. Stick slip actuators are a member of inertial drives family. These actuators can provide large travel distances , high positioning accuracy and high speed [18] [32] [19]. In [33] the authors used input shaping to actuate the stick slip actuator with lower frequencies. These actuators typically use piezo actuators which results in motion in a number of steps to travel long distances. Sub step motion is also available for fine displacement. The detailed working principle of these actuators are discussed in the chapter 4.

In [34] the authors presented a model considering the linear dynamics , hystericus model and the friction model of end effector. In [35] a Neural network based model predictive control was developed for a stick slip micro positioning application. The described control system was able to perform the track the reference position with an accuracy of $0.03\mu m$. In [36] authors presented a neural network based controller for a piezoactuated stick slip actuator.

In [37] [2] the authors have developed a proportional derivative control by using

the voltage and frequency variable for a stick slip controller. The resultant system has an accuracy in the order of millimeters. A PID based control for stick slip actuators was discussed in [38]. The tracking error for the system under discussion was $1.57\mu m$. Cheng et al [39] presented an observer based tracking control for a stick slip actuator. Also GU et al [40] have discussed the design of a piezoelectric stick slip actuator.

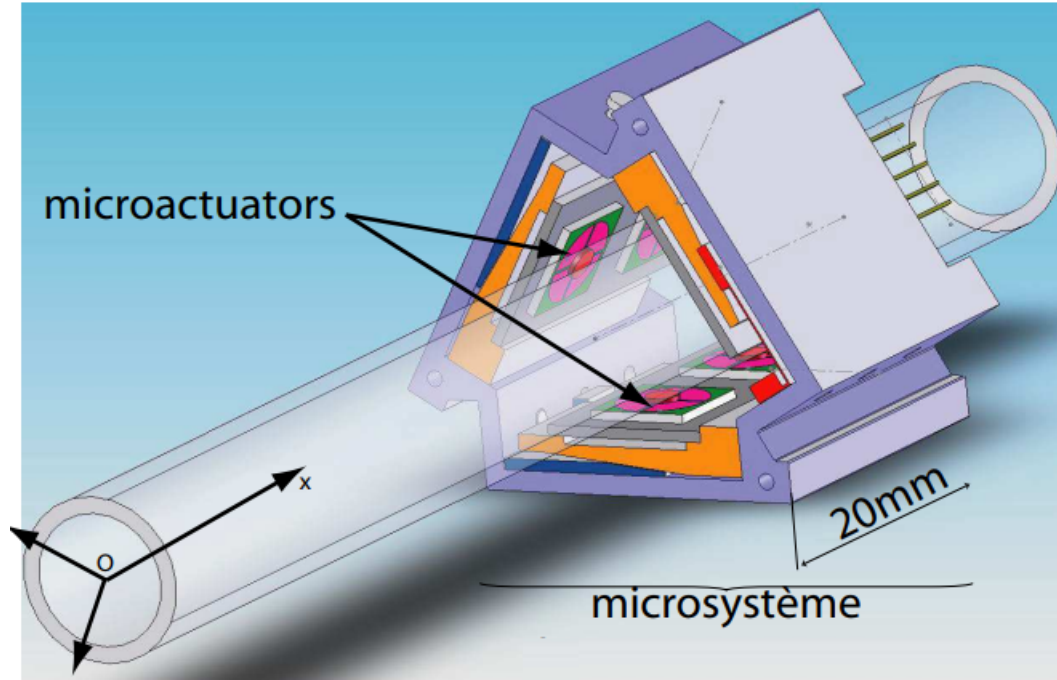


Figure 1.3: Stick Slip Actuator construction used in [2]

In this Thesis we have used SmarAct liner positioners which worked on the stick Slip actuation mechanism. [41–43]

1.1.2 Sensor

Sensing the laser beam position is an important task for free space optics system.

Following types of laser beam detection mechanisms are used in literature.

- Photo Diodes
- Vision Based Beam Spot Detection
- Charged Coupled Devices (CCD)
- Photo Sensitive Detectors (PSD)

The most cheapest and easiest way to sense the laser beam is to use a single photo diode or light dependent resister (LDR) which will give us a boolean 1 when laser beam spot is at the photodiode otherwise it will give us zero. In [3] [1] authors used an array of 4 photo diode to find the laser beam spot position. This system of sensing allows them to tell the location and the direction of laser beam. The photodiode array used for laser beam spot detection can be seen in figure 1.4.

A vision based calibration method for a laser beam tracking system was discussed in [44]. Charged Coupled Devices (CCDs) are also used to measure and detect the laser beam position detection. A CCD is an Integrated circuit (IC) on which an array of small light sensitive elements (called pixels) are placed. These pixels will tell us the position of the laser beam. In [45] [46] the authors have used

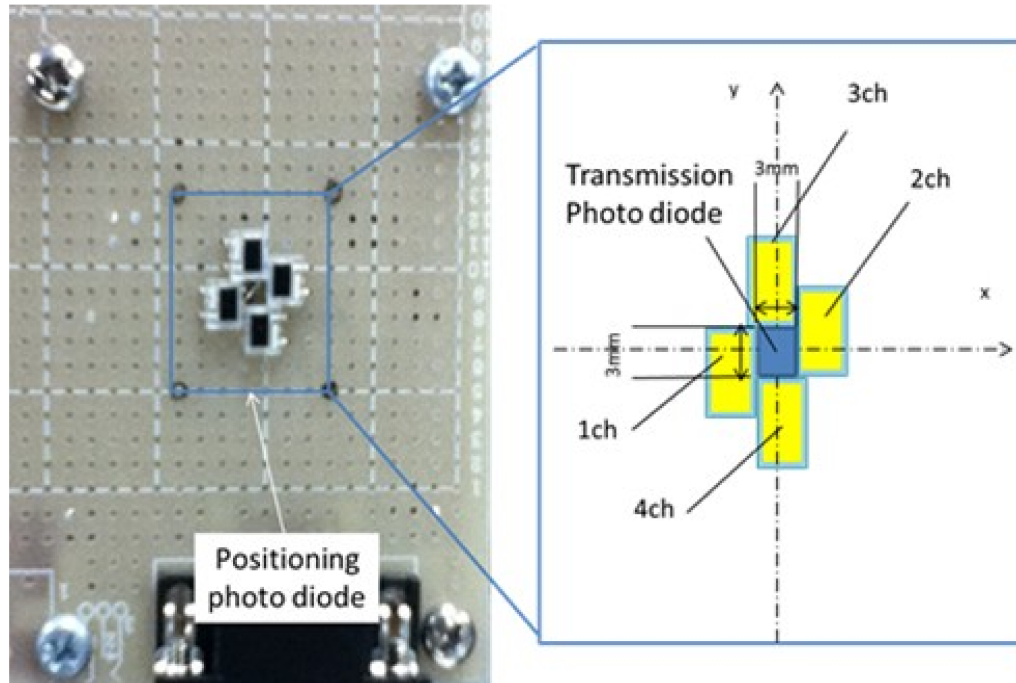


Figure 1.4: Receiver photodiodes arrangement [3] [1]

a CCD to detect the laser beam spot position.

The most common method to detect the laser beam spot is to use Position Sens-

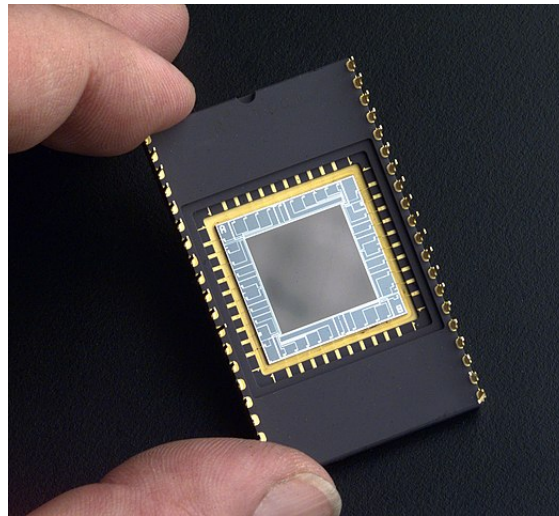


Figure 1.5: A Typical Charged Coupled Device (CCD) sensor

ing Detector (PSD)1.6. Position sensing detector also comprises of four-quadrant photo sensors. These sensors will generate a voltage whenever a light of a specific

wavelength is shone on it. Each quadrant will generate a voltage proportional of the amount of directed beam. The differential voltage will tell us the location of the laser beam spot. The detailed working of the four quadrants PSD is discussed in chapter 2. In [6] an optical position sensor is used to measure the laser beam position. In [5] the authors used PSD for laser beam spot position measurement. Similarly in [4] two Position Sensitive Detectors (PSD) were used to measure the laser beam spot position measurement. Similarly PSD was used to measure the laser beam spot position in various other studies [30] [21] [11] [17].



Figure 1.6: A Photo Sensitive Detector

1.2 Controller Design

In literature several control schemes were implemented for the free space optical communication. In this section we will discuss a brief review for the controller design that is used for the control of free space optics system. Several control

algorithms like feedforward control, PID control , neural network based control, iterative learning etc were used for various types of actuators and sensors.

Model less controllers are the most used controllers for such application. In [1] S.Muta et al uses a proportional type control as described in equation 1.1 and 1.2. The experimental setup is shown in figure 1.2 Here θ_x and θ_y are the mirror angles for horizontal and vertical motion respectively. k_x & k_y are their gains and V_1, V_2, V_3, V_4 are the diode voltages.

$$\theta_x(t) = (V_1 - V_2)K_x + \theta_k(t - 1) \quad (1.1)$$

$$\theta_y(t) = (V_1 - V_2)K_y + \theta_k(t - 1) \quad (1.2)$$

Using the proportional type controller and the scheme mentioned above S.Muta et al [1] was able to successfully follow the receiver travelling at 320 mm/s with the accuracy of 1 mm. The system was successful in transmitting data with 0.5 Gbps broadband transmission. the amplification circuit diagram of the photo detector is shown in 1.2

Tsujimura et al [3] uses a similar technique. They divide the tracking problem in two parts i.e. transient state and steady state. The transient state of the FSO system means that the data transmission is not established yet and the laser transmitter is scanning for the desired position (receiver position). Once the photodiode present at the receiver end confirms the luminance form laser source, steady state

for laser occurs and the data transmission can be resumed. By using the proportional control they were able to successfully track the moving receiver. They proved that long distance transmission is possible even with perturbation in receiver position [3]. For long ranges and non laboratory environment receiver position may experience some perturbations. Thus by using the methodology discussed in [3] reliable connection is ensured.

Jitter rejection is an important problem in FSO systems. Jitter is the variation in the signal due to various external factors such as mechanical movement. Yoon et al [4] proposed a new algorithm for jitter rejection in FSO systems. They have discussed various techniques such as "least quadratic gaussian feed back controller with integrator" , "anti-notch filter" to reject vibratory disturbances [4]. They proposed a "Filtered-X Recursive least square(FXRLS)" algorithm for better performance.

Yoon [4] concluded that the Filtered-X Recursive least square FXRLS adaptive filter , with bias estimator provides superior results as compared to conventional LTI controllers and filtered-X Least mean square FXLMS filter. The schematic diagram of the experiment is shown in Figure 1.7. Zhu [5] proposed a steering mechanism for laser beam using "Fast steering mirrors(FSM)" using piezoelectric stack actuators. In laser beam control we need very fast and precise motion of actuator to achieve perfect tracking. Zhu [5] developed a mathematical model for FSM and hysteresis model for hysteresis representation.

The authors used two types of control schemes. The first one is feedforward



17

of FSM and laser beam was accurately traced by the hybrid controller.

In [27] the authors discussed a solution for the aligning, tracking and positioning(ATP) problem of the laser beam in free space communication. Authors used the steering of the tip tilt mirror (TTM) to maintain the link of the incoming optical beam. The setup require fast movement of the laser beam such that communication link is not broken. To mitigate the waveform aberration in a long distance link they used the Deformable Mirror(DM) and Shack-Hartmann wave front sensor (SH-WFS).

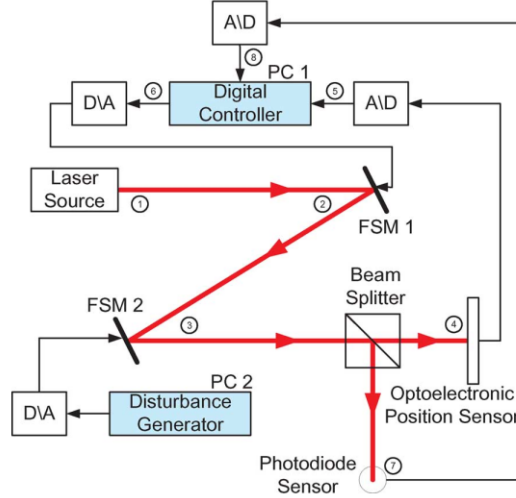


Figure 1.9: Optical path schematic used in [6]

In [6] the authors presented a method of steering the laser beam using only the light intensity as feedback parameter. The schematic path and the experimental setup is shown in Figure 1.9 and 1.10 respectively. A feedback-controlled optical path was designed using a single photodiode sensor to control the light intensity. In their experiment microelectromechanical steering mirrors and

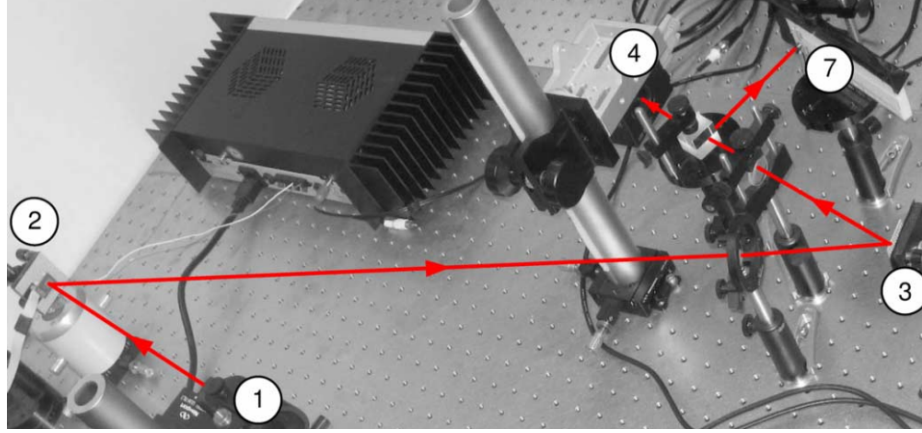


Figure 1.10: optical path used in [6]

standard optical position sensors are used to actuate and control the optical path. The authors showed that this optical system can be modeled as a nonlinear Wiener-Hammerstein polynomial system. They proposed an observer based control scheme. They explored the issue of multiple experiment observability of the non linear optical system and the possibility of the employing the extended kalman filter(EKF) algorithm as a base for designing an observer for the chosen control scheme.

In [47], authors presented a method to cater the both angular and linear drift in a laser beam tracking system. James [28] proposed a model for dynamic mirror actuator employing explicit piezoelectric stack actuator charging dynamics.

Piezoelectric materials mostly have hystereses. There is a need to find some mechanism to model and reject this hysteresis. In [48] author presented a preisach model for the tracking control of piezo-ceramic and an inverse preisach model using feedback control. Similarly [49] presents a lumped parameter based real time representation of piezoelectric stack actuator.

Wei et al [7] developed a new 2-D Fast steering mirror based on piezoelectric actuator. Their structure is shown in 1.11. Each FSM is derived by three amplified

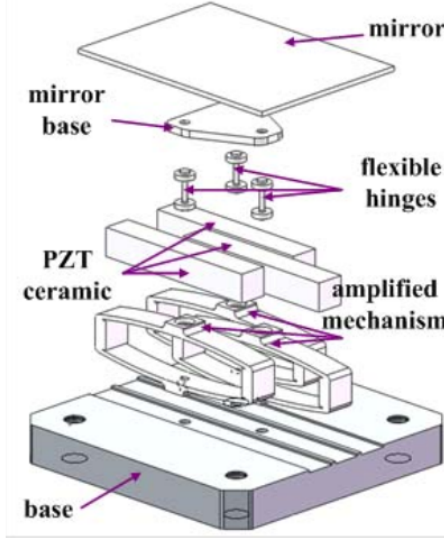


Figure 1.11: Exploded view of FSM in [7]

piezoelectric actuators (APA). Due to their asymmetric structure the driving point of the FSM becomes closer than symmetrical structure of the similar product which makes their design more space efficient. After testing they found out better linearity, high angle, compact structure and fast scanning speed.

Piezoelectric fast steering mirror (PSFM) is widely used in precise control

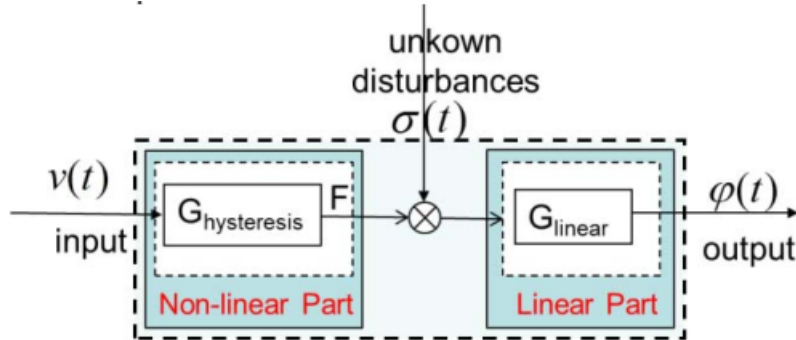


Figure 1.12: precise model of PSFM [8]

application however owing to the hysteresis nonlinearity it is difficult to predict its movement by a conventional linear model. G. Wang [8] tackled this problem in his work. They treated PSFM as a second order system with hysteresis disturbances as shown in 1.12

In [20] the servo design of the 3-D laser tracking measurement signal was conducted. In this study the authors found the relation between the quadrature sensor measurement signal and the required mirror rotation. The authors used the H_∞ optimization for the control. They shown that the required angular movements of the tracking mirror depends upon both the orientation and the distance of the target point. They showed that the frequency domain specification could be introduced directly with the linear system model. Most fast steering mirror that are used in FSO system uses a piezoelectric/piezoceramic material.

[50] The authors used the robust adaptive controller on the system shown in 1.12 and compared this result with PID controller. They selected two kinds of periodic waveforms as the desired trajectories. With Robust adaptive control they discovered the maximum error to be about 210 urad at the beginning and after 0.15 second the steady state value of the peak occurs at about 50 urad. They also implemented a popular PID controller on the same setup and find out the peak error to be 170 μrad and 210 μrad for two different reference trajectories. since the authors considered both the hysteresis and disturbances in their model which lead to a better tracking. A Fractional order PID scheme for the laser beam pointing and

stabilization was discussed in [24]. In this experiment the authors used Position sensing detector (PSD) to get the position feedback of the laser beam spot. They implemented the Fractional order PID (FOPID) scheme and compare this control scheme with the conventional PID and Robust PID methods. According to their experiment the fractional order PID (FOPID) gives better results then PID and robust PID [24] [51] [52]. FOMCON ,A toolbox for using the fractional order control is discussed in [53], [54]. System identification using fractional differentiation models describes/identifies the system more accurately [55] [56] .In [57] authors applied a fractional order PI control for laser beam tracking application. Their Desired system was able to track the system with a steady state error of 0.00003m. A sliding mode based technique was developed in [21]. They applied a variety of continuous time sliding mode control on a free space laser optics system. They compared asymptotic sliding mode controller including an integral term with the conventional super twisting algorithm. Authors used Lyapunov's stability criteria to find the gains of the controller. They concluded that the super twisting algorithm gives us better results than the asymptotic sliding mode controller. Another sliding mode based technique was discussed in [58] by using laser interferometry to control the position of a multi rotor system. Authors compared the sliding mode control with a conventional proportional derivative type controller and concluded that Sliding mode control gave better results than PD controller. In [30] Hui chan developed a closed-loop control of a 2-dimensional micro electromechanical (mems) micro-mirror to be used in a laser scanning microscope. In this experiment

the goal is to control and the micro mirror such that the scanning and imaging performance of the system is improved.

A vision based laser beam tracking system was introduced in [44]. Authors present a calibration method for vision based laser tracker system. By using this method authors easily calibrated the laser beam tracking system which can be further used in a FSO system.

1.3 Proposed Control Method

Free space optics system requires a reliable , highly precise control mechanism. In literature many solutions were proposed to solve this problem. We have chosen the Stick Slip Piezo Actuators (SSPA) due to its large movement range , high accuracy and simple construction structure. Several control schemes were introduced for stick slip actuators. However most of the work was done by controlling the voltage amplitude or the frequency of the input voltage [2] [33]. In this study we have chosen the steps as a control variable and while keeping the voltage amplitude and frequency fixed at a particular level we have controlled the position of the end effector of the stick slip piezo actuator.

In most Free Space optics applications, Photo sensitive detector , photo diodes and charged coupled devices are used to sense the laser beam position. Though these sensors provides good results , they are expensive and the sensing area is very limited. A simpler method to sense the laser beam position was introduced by using a camera. The camera was able to detect the laser beam position correctly.

We have also used the labview model identification toolbox to identify the system model. By using the identified system model we can apply the model based control algorithms. Iterative learning control and fractional order PI control was also investigated and simulated on the identified plant model.

1.4 Thesis Organization

This document is divided mainly into four chapters. The first chapter includes the introduction of the research problem and discussing the existing work done in the controlling of free space optics. In the second chapter, we will discuss the overview of the experimental setup that we are going to use. In the third chapter, a vision based laser beam spot tracking mechanism is discussed. The fourth chapter is dedicated to the feedback control of the stick-slip piezo actuator. In the last chapter, we have discussed the conclusion and future recommendations.

CHAPTER 2

EXPERIMENT LAYOUT

The experimental setup that was initially proposed is shown in figure 2.1. For

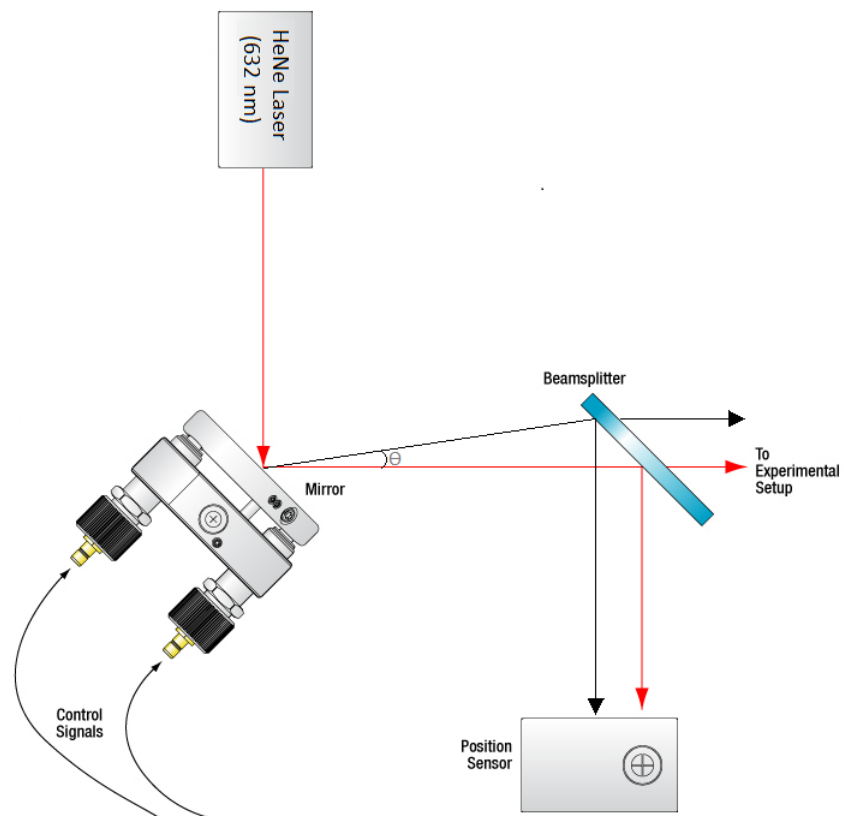


Figure 2.1: Experimental Setup

this experiment, we used the equipment from Thorlabs and SmarAct. The main idea is to transfer the data using a laser beam. This data is received by a special laser receiver which can obtain the modulated data from the laser beam. However, due to the very small size of the receiver, a small perturbation in the laser transmitter will lead to very large displacement in the laser beam position on the receiver plane. To measure the position of the laser we will use the position sensor PDQ80A. Since PDQ80A does not allow the laser beam to pass through itself, we used a beam splitter to split the laser beam into two parts. Beam splitter passes most photons through itself and reflects some of the photons at a particular angle. This reflected beam is then directed towards the position sensor while the other beam which is passing through the beam splitters directed towards the laser receiver. As explained earlier, the idea of this study is to stabilize the beam to a certain fixed reference point such that a reliable connection between the laser transmitter and receiver is maintained. We can use National Instruments myDAQ to get the input/output analog and digital signals and use them accordingly in a LabVIEW program / Virtual instrument (VI).

Since the PSD has a very small sensing area, an image processing based approach was used where we used a camera as a laser sensor. A color detection based algorithm was used to identify the position of the laser beam spot and using the position of the laser as feedback to the system, consequently steering the beam position towards the desired position. For color detection, it is important that the lighting conditions and environmental noise does not change while performing the

experiment. Thus this algorithm is best suited for a controlled lab experiment. We used a servo motor to move/ steer the laser beam. The servo motor has an angular range of 0-180 degrees. To control the servo motor we have used the Matlab support package for Arduino. Initially, the experiment is performed with only one servo motor thus the system has only 1 degree of freedom(DOF)(vertical). The hardware setup used for the experiment is shown in figure2.2. A special black cloth is used as the background to get better contrast and to minimize the laser beam spot reflection.

Although the servo motor is a good solution to steer the beam inside the sensing

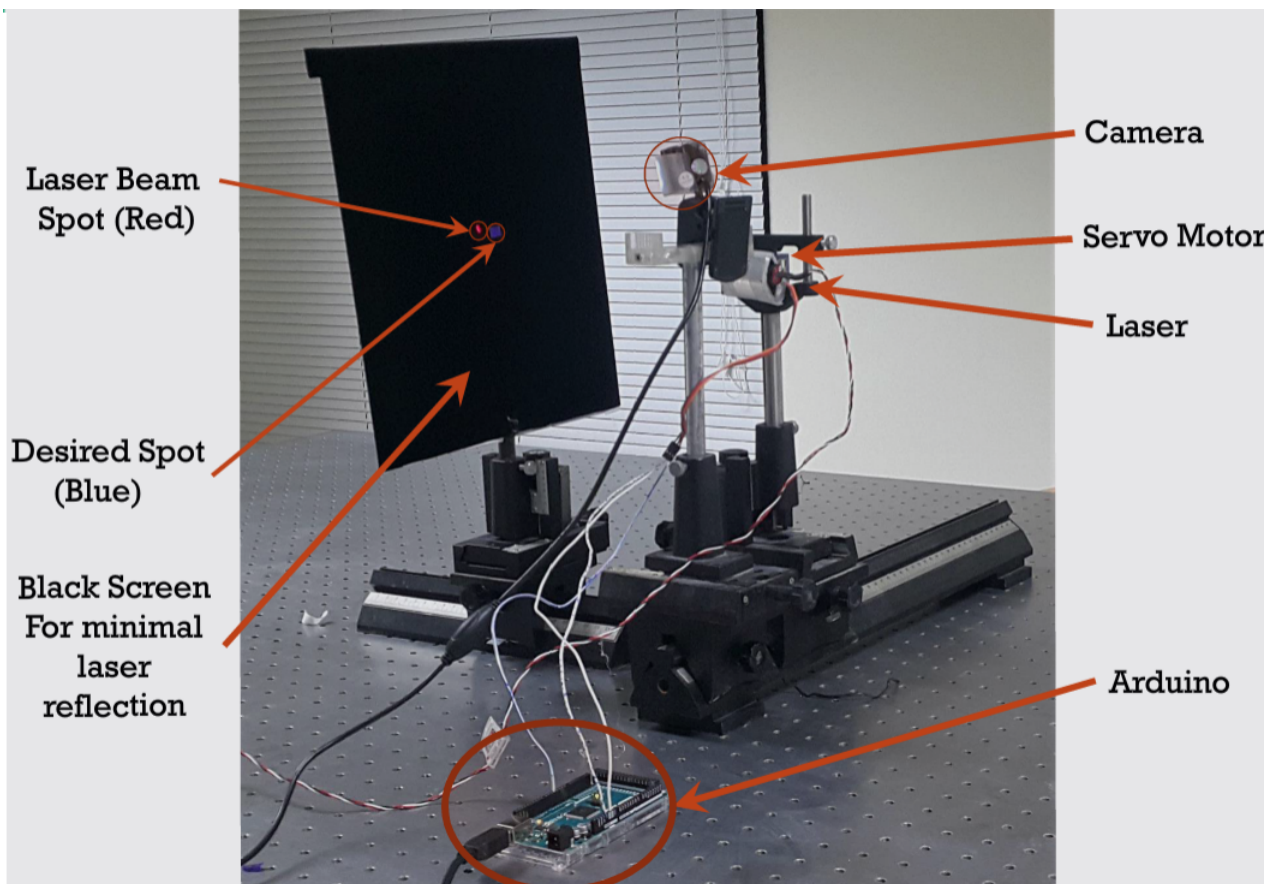


Figure 2.2: Color Detection Setup

area, the angular resolution of a servo is not good enough. Since we require much better accuracy to establish a reliable wireless optical connection between laser transmitter and receiver, we will use a piezo electric mirror mount which has a much better accuracy. As shown in figure 2.3 the servo is used to steer the beam inside the sensing area of PSD and the piezoelectric mirror mount is used to steer the beam towards the center of the target.

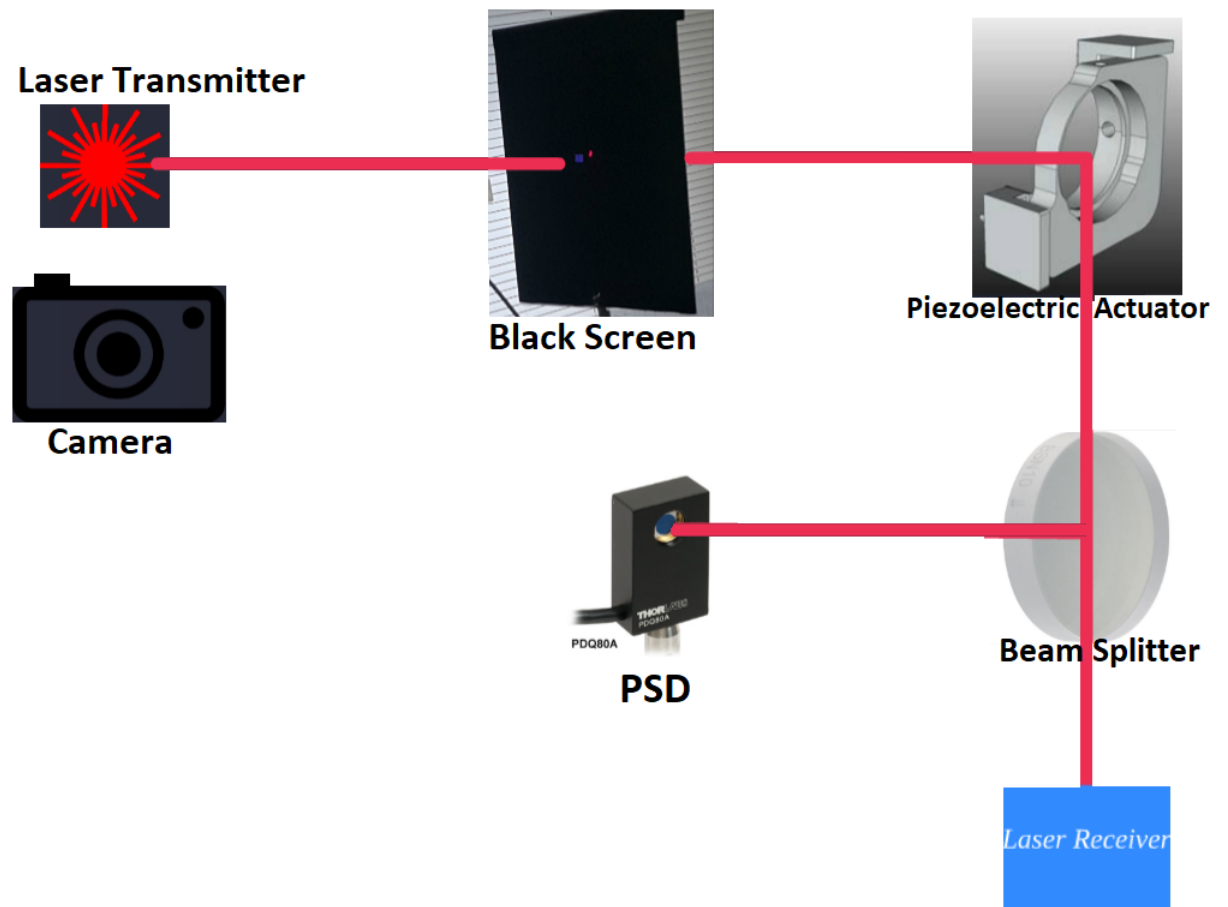


Figure 2.3: Complete Experimental Setup

In table A the list of main parts that were used in this experiment is stated. various other fixtures , cables and other small parts were also included however in this section we will discuss the working and introduction of these main parts.

2.1 Helium-Neon Laser

In Free Space optics communication such as this experiment we need to transfer the data in using visible light. Due to its focused beam and very low beam divergence lasers are the obvious choice as data carrier. For the current experiment we choose Thor Lab's Helium-Neon Laser HNLS008L. This laser emits red laser beam of wavelength 632.82 nano meters. HeNe Lasers have a chamber



Figure 2.4: HeNe Laser beam

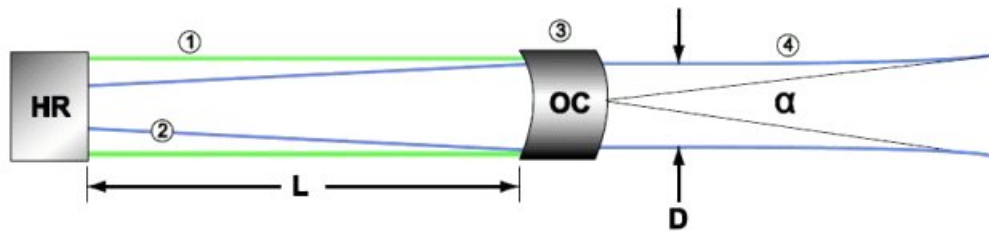


Figure 2.5: Optical Resonator Cavity

consenting Helium and neon gas under low pressure at a particular Helium Neon ratio ranging from 5:1 to 20:1. When voltage is applied to this gas chamber with anode and cathodes on both ends electrons collide with helium atoms resulting

in excitation of helium atoms 2.5. These helium atoms than collide with neon atoms resulting in an excited state of these neon atoms. Excited neon atoms keeps on building until population inversion is achieved. This excitation results in emission of light photons having 632.82nm wavelength.

Several other wavelength are also emitted during this process for example 3.39 μ m and 1.15 μ infrared light , and a variety of visible spectrum light including green yellow orange and yellow orange light. We can use correct mirror and lenses to extract the light of desired wavelength

Typical HeNe Parameter	Value
Beam Diameter	1 mm
Full Angle Beam Divergence (α)	1.5 mrad
Cavity Length (L)	0.15 m (0.5 mW) to 1 m (35 mW)
Reflectivity at High Reflector (HR)	> 99.99 percent
Transmission at Output Coupler (OC)	1 percent

Table 2.1: Typical HeNe Parameters

The typical parameters of HeNe lasers are given in table 2.1. The laser that we are using HNLS008L does not have perfect beam collimation. it has a full angle beam divergence (α) as 1.5 mrad. due to this beam divergence the diameter of the beam keep on increasing with the increment on distance. Thus if the operating distance of laser is very large we might need a variety of lenses to collimate the beam at the receiving end.

2.2 Position Sensor

We require a precise laser beam detector to measure the position of laser precisely. for this we use Thor Lab's PDQ80A quadrant laser beam position detector in Fig 1.6 As seen in 2.6 the PDQ80A has 4 quadrants sensing regions which are sperate from each other with a small distance. as the beam falls on the sensor, these sensors gives voltage according to the intensity of the beam falling on each quadrant.

The sensing range of this sensor is between 400 to 1050 nm wavelength. which fits well with our application since we are using 632.82 nm wavelength laser. However due to the spacing in the sensors it is recommended that the beam spot diameter should be limited between 1mm to 3.9mm such that it does not cover the whole sensor or the beam spot size is too small for the sensor to measure.

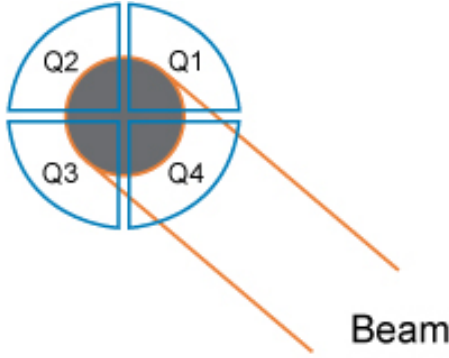


Figure 2.6: PDQ80A sensor placement

The PDQ80A have 6 pins whose functions are illustrated in table B. Three major signals are given out from this sensor which are "XDIFF" , "YDIFF" and "SUM". XDIFF is the difference of voltages between horizontal axis i.e.

$$\text{XDIFF} = (Q_2 + Q_3) - (Q_1 + Q_4)$$

$$YDIFF = (Q_1 + Q_2) - (Q_3 + Q_4)$$

$$Sum = Q_1 + Q_2 + Q_3 + Q_4$$

here Q_1, Q_2, Q_3 and Q_4 are the photocurrents of their respective quadrant sensor. to get the x and y position of the beam we will use the sum value to normalize the XDIFF and YDIFF value.

$$X = \frac{(Q_2 + Q_3) - (Q_1 + Q_4)}{Q_1 + Q_2 + Q_3 + Q_4} = \frac{XDIFF}{Sum} \quad (2.1)$$

$$Y = \frac{(Q_1 + Q_2) - (Q_3 + Q_4)}{Q_1 + Q_2 + Q_3 + Q_4} = \frac{YDIFF}{Sum} \quad (2.2)$$

Thus by using equations 2.1 and 2.2 we can find the coordinates of the beam spot on PDQ80A.

PDQ80A is not manufactured to be a stand alone device, the manufacturer recommends to use another controller KPA101 to acquire and control the signal from PDQ80A.

2.3 K-Cube Position Sensing Detector (PSD)

Auto Aligner

KPA101 position sensing detector PSD auto aligner is a compact solution which is used to integrate/control the Position sensor PDQ80A . This motion controller came with its own softwares named Advanced Positioning Technology (APT) and Kineses. These software provides a graphical user interface in which we can easily read and write data from the KPA101 auto aligner. We used the Advanced

Positioning Technology (APT) software to connect and acquire the data from auto aligner.

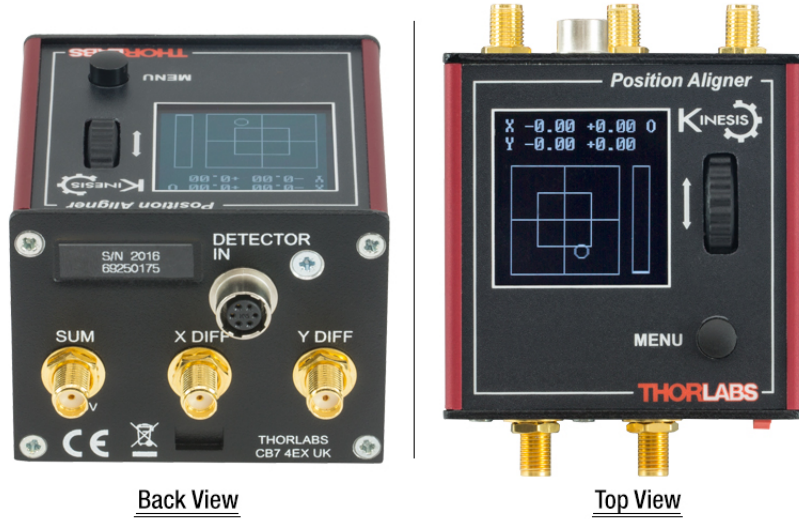


Figure 2.7: KPA101 Auto Aligner

KPA101 is an interface to connect directly the signals from PDQ80A to software. This auto aligner has three basic modes i.e. open loop mode, monitor mode and close loop mode. By selecting the appropriate mode we can either measure the x-diff and y-diff values or the normalized x and y coordinate value or we can get the control feedback respectively. We can select these modes directly from the top panel given on KPA101 or by selecting the respective options from APT software. When used in the closed loop mode the KPA101 will give control output which can be directly be fed to the piezo actuator controller such as KPZ101.

Advance Positioning Technology or APT software which is provided with KPA101 is compatible with ActiveX technology. ActiveX is Microsoft developed

technology which helps in linking one program with another. Since we are using LabView to control the process we can use the ActiveX control in LabView to call the APT software inside the LabView environment. In LabView we can write our own program to acquire or manipulate the data given by APT according to our needs.

2.3.1 PINs Overview for Auto Aligner

KPA101 provides various options to input/output data. We will discuss briefly the function of each pin in KPA101 in this section. In this auto aligner we have 5 SMA connectors as shown in figure 2.8.

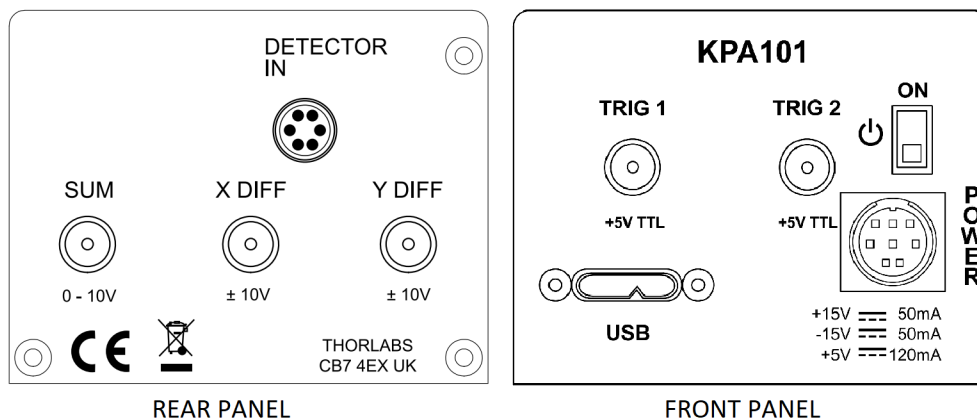


Figure 2.8: Connections on Front and rear panel of KPA101

SUM

Placed on the rear panel, the SMA connector for Sum value gives the Sum value/Voltage from the quadrant position sensor.2.8

XDIFF

Placed on the rear panel, X-diff In open loop gives the X-diff value of PDQ80A quadrant position sensor. In Close loop this connector gives the control feedback for x-axis.

YDIFF

Placed on the rear panel,Y-diff in open loop gives the Y-diff value of PDQ80A quadrant position sensor. In Close loop this connector gives the control feedback for Y-axis

Trig 1 , Trig 2

Trig1 and Trig 2 SMA connectors are placed on the front panel of KPA101. They are bidirectional trigger ports which operates on TTL logic.These ports detects the voltage below $+0.8V$ as logic LOW and the voltage above $+2.4V$ as logic HIGH.we can adjust the triggering of these ports for example logic LOW/HIGH or Falling/Rising Edge triggered according to our application.

These ports can be used as either input or output according to our choice. There are different modes options available depending upon the choice of Trig1 and Trig2 e.g. Disabled , Digital Input, LLGetStatusBits method , Trig IN: Loop

Open/Close , Digital Output , Trig Out: Inside Sum range , Trig Out : Below Diff Threshold , Trig Out:Sum and Diff Combined. These modes have their own operation can be chosen according to our need.

2.4 Mirror Actuator

Figure 2.9 shows the front and back view of the mirror. We used Polaris k1PZ 3-axis piezo mirror mount. The presence of piezoelectric element in this actuator allows us the movement in three axis with very small angular resolution. With a step size of 0.1 Volts we can obtain the angular movement of $0.5 \mu rad$. which means that for 0.1 volts 0.000029 degree is the resolution and the range of piezoelectric is $500 \mu rad$ or 0.029 degrees. With this small resolution we can move the laser beam with high precision.

The Piezoelectric material used in this mirror mount operates at a high voltage



Figure 2.9: 3-axis Piezo actuator (front and back view)

range of 0-150 Volts. It uses 3 BNC cables to deliver the control voltage

2.5 Open Loop Piezo Controller MDT694B

We require a high voltage controller to deliver the high voltage to the piezo actuator. MDT694B is a precise and high voltage open loop controller. MDT694B is a

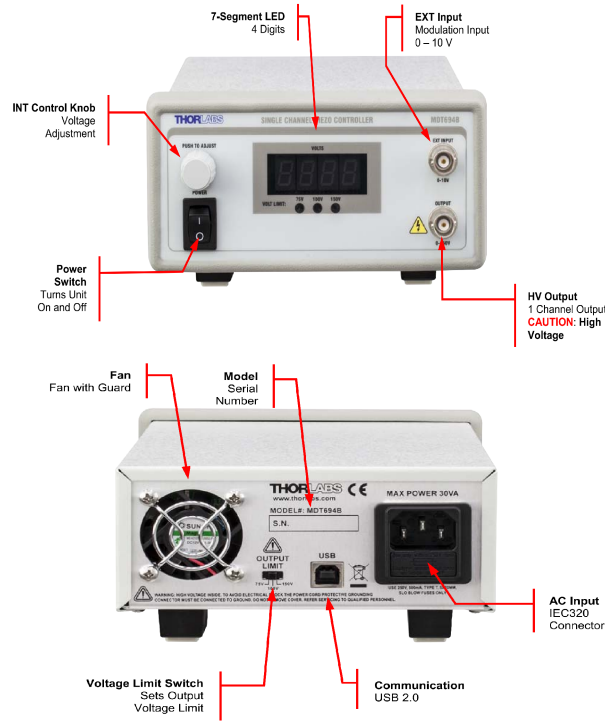


Figure 2.10: Open-loop Piezo Controller

single channel open piezo controller. It can control one axis of the piezo mirror through its BNC connector. It can give the output voltage up to 0-150 volts. It has three maximum voltage limit settings. MDT694B has a select switch on the back side from which we can select 75 volts, 100 volts and 150 volts maximum voltage settings. If we choose 150 volts then the output voltage can be found by using the following equation. 2.3

$$V_{out} = V_{manual} + 15V_{external} \quad (2.3)$$

here we can apply an input voltage from 0-10 Volts to the EXT BNC input on the front panel. Thor labs also provide a compatible software from which we can control the voltages applied through MDT694B using a graphical user interface (GUI).

2.6 Beam Splitter

Beam Splitter is a device which splits the incident light beam into reflected and transmitted beam. We used the Beam Splitter BSF20-A. This beam splitter is a plate type UV Fused silica Beam splitter. on One side of the BFS20-A Beam splitter there is AR coating to prevent unwanted reflectance.

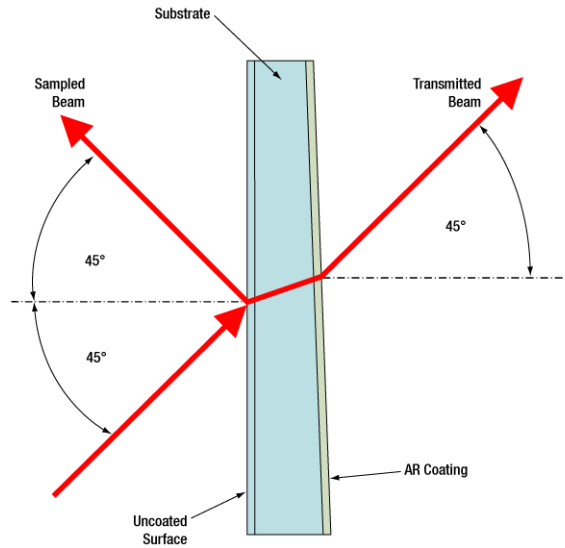


Figure 2.11: Beam Sampling

As we can see from figure 2.11 Incident light is divided into two portions one is reflected back at a particular angle and the other one is transmitted through the

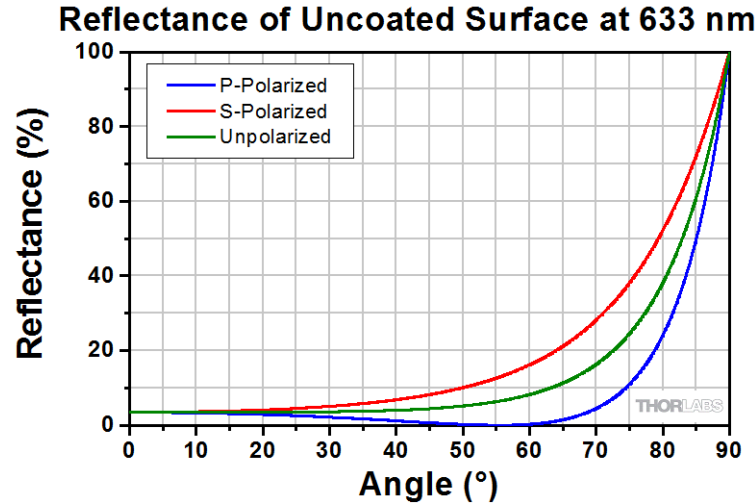


Figure 2.12: Beam Sampler reflectance graph as provided by manufacturer

beam splitter. The BFS20-A beam splitter induces an offset in the transmitted beam. The reflectance of the beam sampler also varies with different angle of incidences (AOIs). We can see the graph of reflectance versus angle of incidence in figure 2.12 for the un-coated surface. From figure 2.12 we can see that for a 45 degree AOI on the uncoated surface, we got the reflection of almost 5 percent for unpolarized light. Also the AR coating is used to avoid reflection so as shown in figure?? we can see that for a laser beam of 632.82 nm wavelength a reflection of almost 0.5 percent reflection.

Although the AR coating is provided to minimize the ghosting phenomenon, in our experiment we still experience ghosting. In Ghosting the laser beam is reflected from both the uncoated and coated surfaces of the beam splitter resulting in two different reflected beam spots. These spots are sufficiently far enough when the distance is larger. Figure 2.14 showed the phenomena of ghosting.

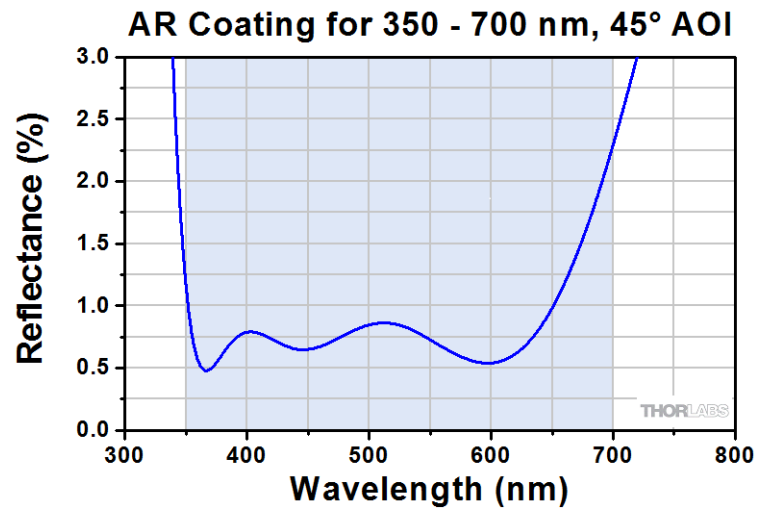


Figure 2.13: Effect of AR coating at 45 degree AOI as provided by manufacturer

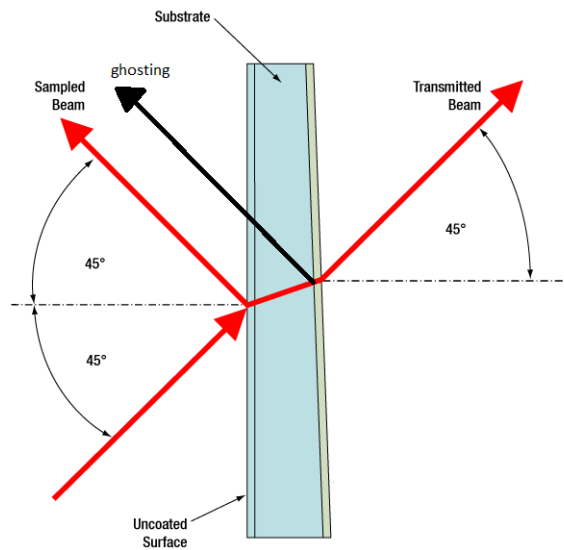


Figure 2.14: Ghosting

CHAPTER 3

LASER BEAM SPOT TRACKING USING IMAGE PROCESSING TECHNIQUES

3.1 Motivation

Precise control of laser beam spot is a very important problem in free space optics (FSO) communication systems. Piezoelectric actuators are a promising way to control the laser beam with significantly higher accuracy. Although the piezoelectric actuators (PA) provides very good movement resolution , they mostly lack the desired movement range without some type of special mechanism . A typical FSO laser beam setup can be seen in figure 2.1. According to this setup a laser beam is directed towards a piezoactuated two dimensional angular mirror. This mirror reflects the laser beam such that it is passed through a beam splitter,

which splits the beam into two separate beams. One beam is directed towards the experiment , while the second beam is directed towards a photosensitive detector (PSD). This PSD gives us the feedback information of the position of laser beam spot.

In this setup we have used the Thor labs PDQ80A photo sensing detector 1.6. The extremely small sensor area limits us to always stay within the diameter of $7.8mm$, which is very difficult when the distance between transmitter and receiver is large.

Thus the main problems identified in the said experiments are the following

- Very Short dynamic range of Piezoactuators
- Low accuracy of motorized actuators
- Very small sensing area of laser beam spot detector

In this experiment we have proposed to use a servo model which have a poor dynamic resolution but the dynamic range is large enough. We can combine the servo motions and piezoelectric motions to get a good resolution and good dynamic range. A solution to the small sensing area is proposed by using image processing techniques to measure the laser beam spot on a dark screen. Thus we can measure the laser beam position on a larger surface area for coarser measurements.

In figure 2.1 the typical experimental setup sketch is shown. In this setup, a piezo actuator is used to steer the laser beam towards the center point. However, this system cannot correct the errors in laser beam position of very large magnitudes.

As shown in figure 1.6 the effective sensing area of Position Sensitive detector (PSD) is $7.8mm$ diameter. Thus a need for some mechanism arrives where we can enhance the allowable laser beam position range.

3.2 Experimental Setup

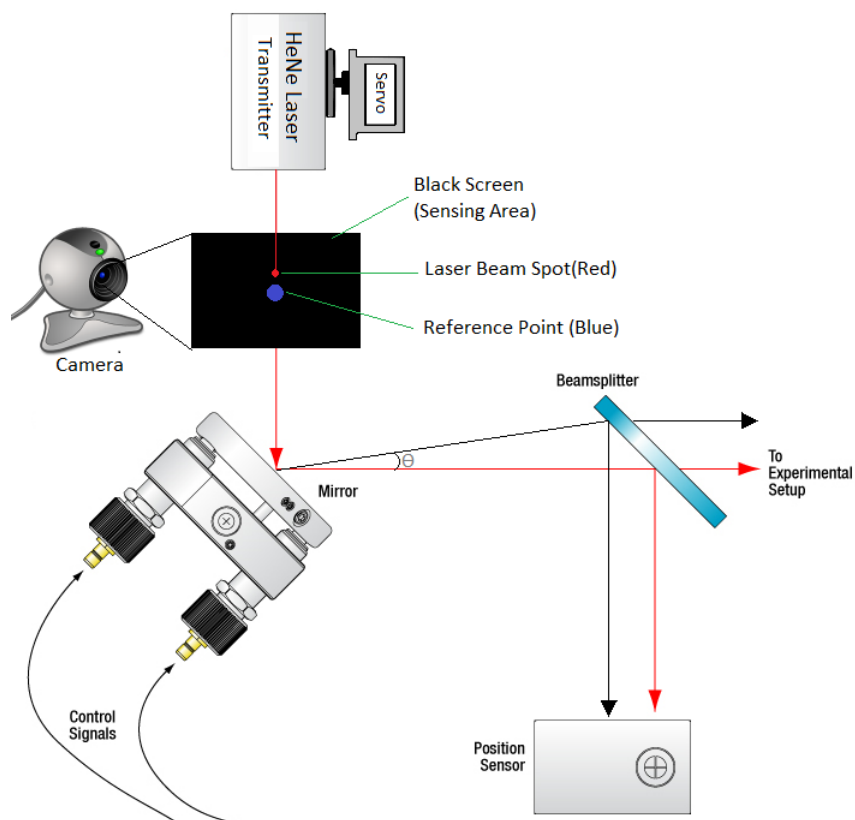


Figure 3.1: Experimental Scheme with Image processing

In figure 3.1 an image processing based solution is proposed. We have attached the laser beam on a servo motor. A Black Screen with a hole in the middle is placed in the laser beam path as demonstrated in 3.1. This Black

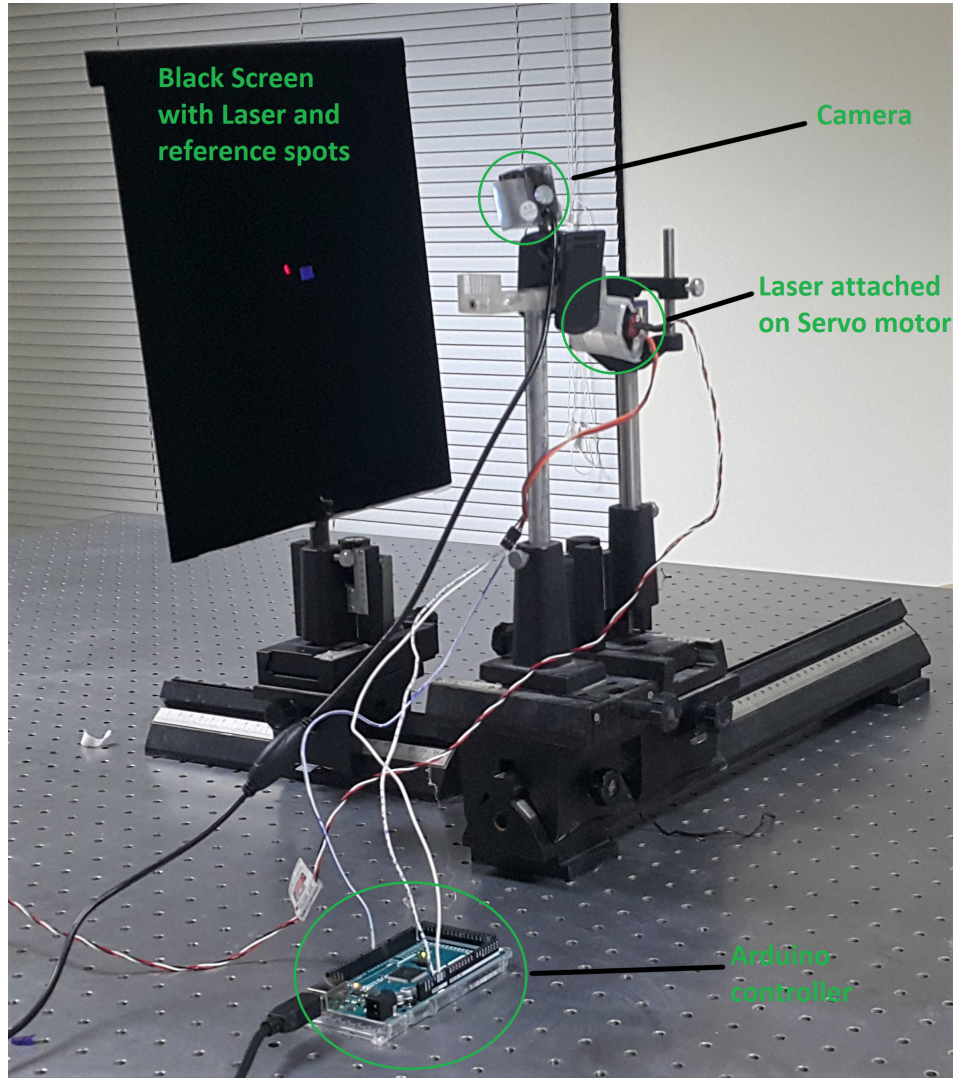


Figure 3.2: Experimental Layout

screen combined with a video camera will serve as a laser beam position detector with higher measurement range. We have fixed the camera in a position such that it captures the desired area on the black screen. A Color detection algorithm was used to measure the position of laser beam and the position of the reference point. Thus by using the feedback from the camera we steer the laser beam towards the desired position. The laser will pass through the hole, and towards the piezoactuators. Thus the camera based color detection algorithm provides

us with an initial alignment scheme for FSO system to increase the movement range. The hardware setup can be seen in figure 3.2

A single micro servo motor is used as an actuator to steer the laser beam. Micro servos does not have high current requirements, thus they can be controlled directly through a micro controller. We used the arduino at-mega micro controller to control the servo motor. A matlab support package for arduino is available through which we can access and send commands to arduino. Micro servo has an angular range of $0 - 180^\circ$. In matlab, when we send arduino a command of 0, it will correspond to 0 degrees and 1 will corresponds to 180 degrees movement. Thus a command between 0 to 1 will correspond to the end effector movement of 0 to 180 degrees. Since we are using a single servo motor, laser beam movement is only limited to one dimensional movement (vertical).

3.3 Color Detection

In this section we will discuss the color detection technique for the identification of laser beam spot and reference signal. The laser beam spot has a color of red while we have placed a hardware reference of blue color on the black screen. A USB web cam is used to capture a continuous video for processing.

From literature we already know that a video is a combination of several images or frames. Each frame is combination of many pixels. And every pixel has a distinct color which is defined by its RGB value. In an RGB image only red green

and blue colors are present in every pixel and the concentration of these primary colors will define the output color of that pixel. For example a completely white pixel color is obtained by setting all the values of RGB to their maximum values i.e. 255. while a complete dark pixel is obtained by setting all the red green and blue values of that pixel to their lowest values which is zero.

Thus in summary an image can be defined as a matrix whose each entry is a pixel which further contains three values of red , green and blue color. If the image has a resolution of 720x480 pixels that means that the image matrix has 720 entries(pixels) in the horizontal direction and 480 entries(pixels) in the vertical direction. From here we can define a X, Y pixel position for every pixel. for example the top left pixel of that image has a pixel position of $xy = (0, 0)$ and the bottom right pixel has a position of $xy = (720, 480)$. Our main goal in this algorithm is to scan for the pixels with most red and blue components and find their pixel position. A Blob means a group of connected pixels in an image. BLOB stands for binary large objects. Here a blob on the position of red pixels will represent the position of laser beam and a blob on the position of blue pixels will represent the reference or desired position

The first step in color detection is the image acquisition from the camera into Matlab. we have used the Matlab image processing tool box for this purpose. Since color detection is a relatively computationally expensive task, it is not possible for us to process all the images in real time. The image acquisition rate



Figure 3.3: RGB Acquired Image

of our camera is 30 frames per second and to process the video in real time, it is better to skip few frames while measuring the position of blobs. So we acquire and process only every fifth frame for this purpose.

.The image resolution that we have set for our experiment is 640x480 pixels. Since the camera will give acquire the mirror image , we flipped the image acquired from the camera.The acquired RGB image is shown in Figure 3.3.

The next step is to convert this image into its gray scale equivalent.This transformation will help us extract the red and blue components of the RGB image. The result of this transformation is represented in figure 3.4.

In the next Step we have to find the differential image for the red color (laser beam spot).This is achieved by subtracting the gray scale image from the Red component image of the acquired frame.The differential red frame is shown in figure 3.5. Now in this image only those pixels who have significant red portion

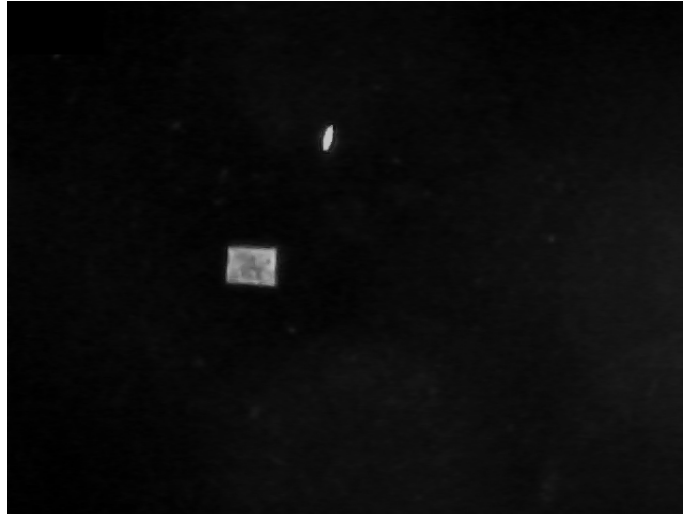


Figure 3.4: RGB converted to Gray Image

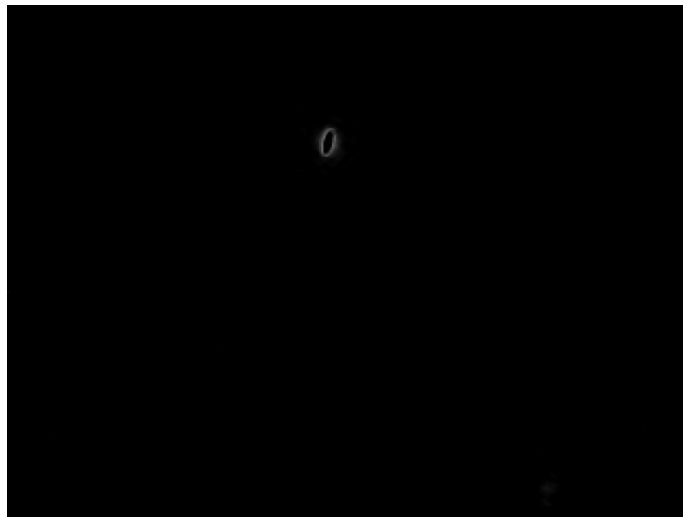


Figure 3.5: Differential Image Red Color

remaining are left. Thus we see a black n white blob where the red beam spot was present and the blue blob is vanished. Afterwords we apply a median filter to smooth out any noises present in the image.

Now we will further highlight the red blob as obtained in the differential red frame. This is one by converting the gray scale image into a binary image. In this

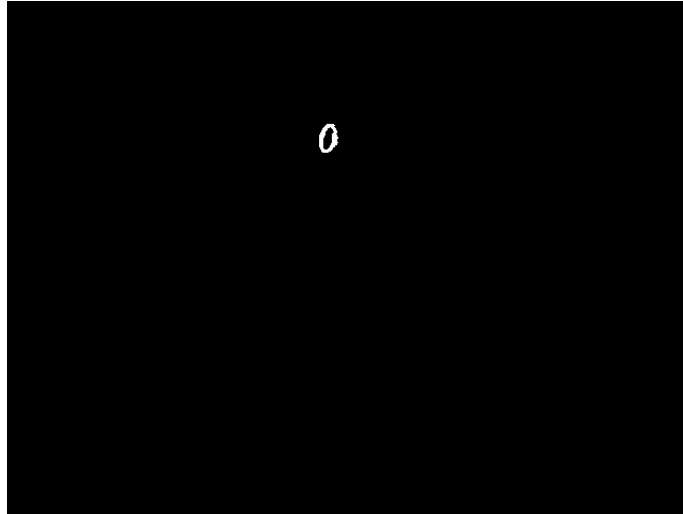


Figure 3.6: Red Objects detected

image we select an appropriate threshold which depends upon the color contrast and external lighting conditions. Any image who has an intensity below this threshold will be treated as a pure black pixel and any pixel which has an intensity higher than this threshold is treated as white pixel. The choice of threshold is very important since a too low threshold may highlight any noise that may present in the image and a very high threshold may ignore the actual red color that is present in the image. The binary image for red pixel is represented in figure 3.6.

The same procedure is applied for the blue color. We use the gray scale image transformation obtained earlier figure 3.4. We obtained the differential blue frame by subtracting the blue component image from the gray scale figure 3.7 . Afterwards we apply a suitable threshold to get a binary image which highlights the blue component of the image figure 3.8.

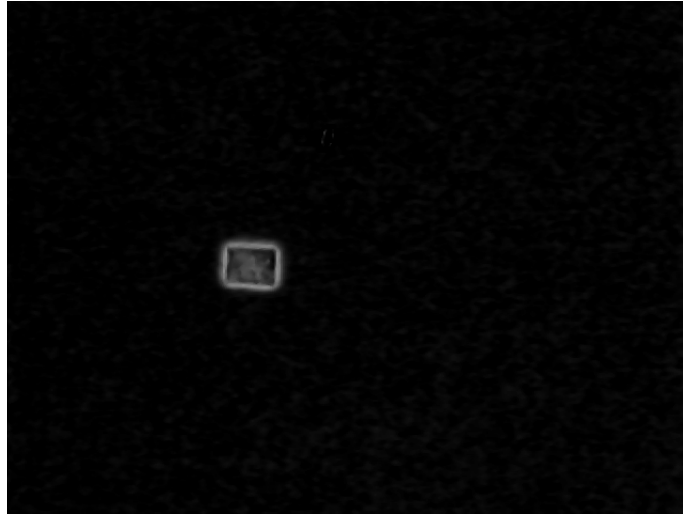


Figure 3.7: Differential Image Blue Color

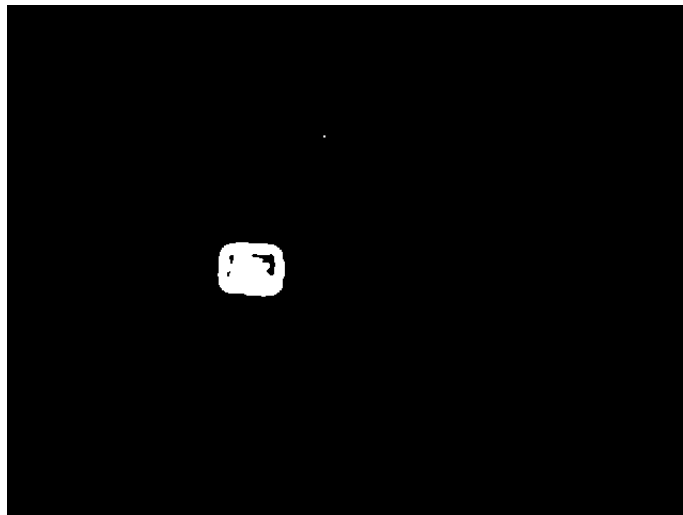


Figure 3.8: Blue Objects detected

After obtaining the binary images for red color (Figure 3.6) and blue color (Figure 3.8) We now apply blob analysis command. In our binary blue and binary red image we expect that the reference point and the lasers are identified as a blob. We have fixed the maximum and minimum blob area to be detected to a suitable number such that neither the whole image is considered as one blob , nor very tiny noises are considered as one blob. moreover since we only desire

one blue blob and one red blob thus we have also limit our number of detected blobs to 1. After identifying the correct blobs we can identify the centroid of that blob in terms of XY point or the pixel position to identify the location of laser and the reference signal on the image. We can draw a rectangle on the identified blob and we have displayed their pixel position on the image. The result of BLOB analysis is shown in figure 3.9 .

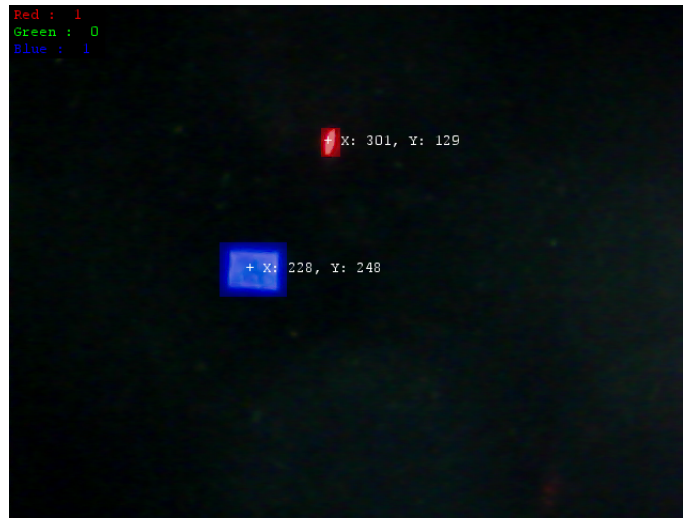


Figure 3.9: Detected Color

The Flow chart of the above algorithm is shown in figure 3.10 .

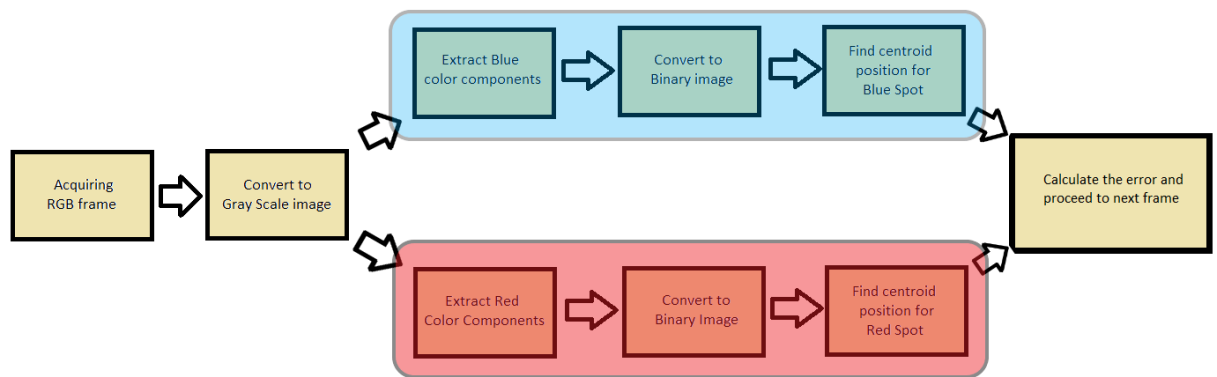


Figure 3.10: Flow chart

CHAPTER 4

FEEDBACK CONTROL OF PIEZO ELECTRIC STICK-SLIP ACTUATOR

4.1 Introduction

In Free Space Optics System (FSO) a main requirement is to establish a reliable contact between optical transmitter and receiver. Due to the very small size of the optical receiver, a very precise control is needed to establish a reliable connection between transmitter and receiver. A conventional DC motor actuation cannot provide the required accuracy in the order of nano meters. Thus we used a piezoelectric material to move the poistioners with a small accuracy. Piezo electric actuators consists of a special materials which apply a force (change its dimensions) when a high voltage is applied to it. The displacement achieved by

applying a voltage could be very accurate due to the absence of gears or other conventional mechanical linkages. However the available piezoelectric actuators provides very poor dynamic movement range due to their physical limitations.

Piezo-actuated stages are becoming more and more popular in the micro or nano positioning applications. Piezoactuators are used in various real life applications where precision is important. Some typical including Atomic Force Microscopes (AFM) [59], Scanning Tunneling Microscope (STM) [60], Machine tools with ultra precision requirements [61] [62] and Free Space optics System [24] [21] e.t.c. Due to the requirement of higher precision in positioning we cannot use the conventional actuators for these application. Some available actuators types for micro and nano positioning are piezoelectric actuators, magnetostrictive actuators, MEMS based Electrostatic actuators, MEMS based Electrostatic surface actuators, MEMS based Electrostatic shuffle actuator, MEMS based electromagnetic actuators, and MEMS based Thermal Actuators [16]. In our particular application in FSM we choose the piezoelectric type stick slip actuator due to their excellent operating bandwidth, precise movement and the ability to generate large mechanical forces for a small power input [16]. However a major drawback of the piezoactuated devices is that they have a very small dynamic range. This problem of small dynamic range can be solved by having a Stick-Slip type Piezoelectric actuator. Thus a Stick Slip mechanism is proposed [18] to increase the dynamic range of the poistioners. We have used smaract linear positioner SLS-5282-L with an integrated sensor [42].

The Experimental setup can be seen in Figure 4.1.

In Free Space Optics(FSO) communication the available Stick Slip Piezo Actuators(SSPA) could be a linear type actuator or an angular type actuator. Both linear type or angular type actuators have their own pros and cons. The linear type actuators are preferred because of their Simple design , Better position resolution , position resolution is independent of the distance between transmitter and receiver. However the linear type SSPA has a limited movement range , and we have to stack two linear type SSPA onto each other which limits the amount of weight that can be placed on to these actuators. On the contrary, the angular type SSPA provides us Better position range and the position resolution and the position range depends on the distance between transmitter and receiver. we can significantly increase/decrease the maximum distance travelled by the laser beam spot by changing the distance between the transmitter and receiver. However the angular type SSPA has a relatively complex design and the resolution and range could add some additional complexity to the experiment. In this particular experiment we have studied the control of linear type Stick Slip actuator (SSPA).The mechanism of piezoactuated stick slip actuators is described in the next section.

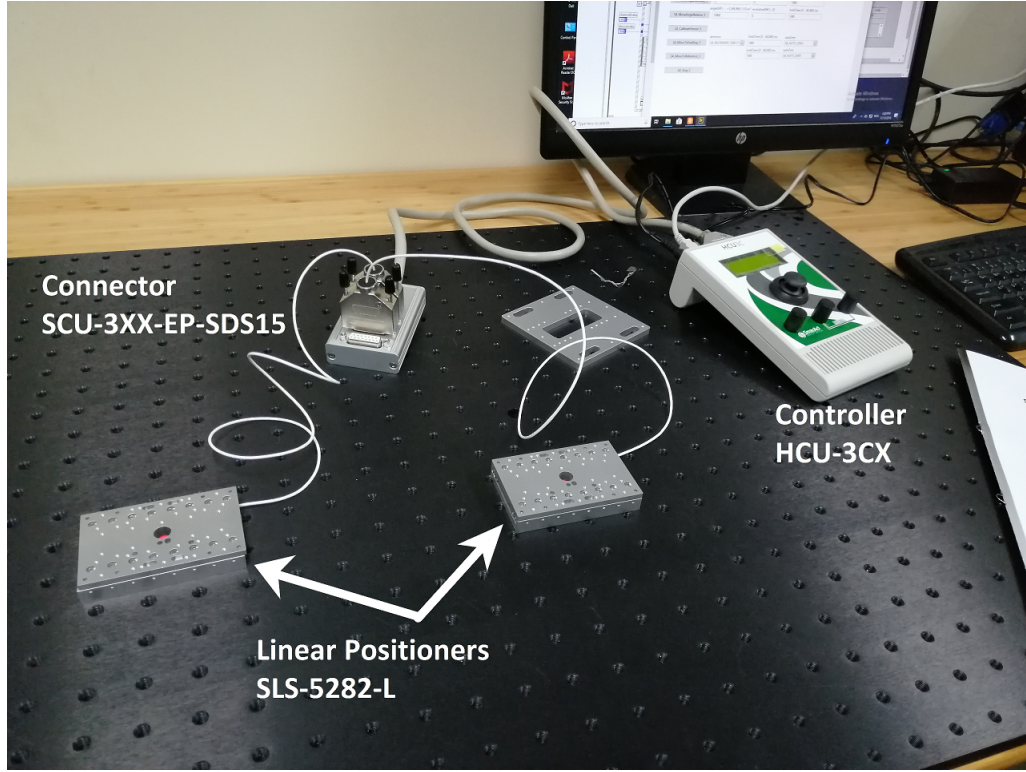


Figure 4.1: Experimental setup

4.2 Working principle

Stick slip mechanism works on the principle of static and dynamic friction. We already know that the static friction is more than the dynamic friction. Assume a cup placed on a very smooth silk cloth. when we slide the cloth with a slow speed, the cup above the cloth also moves along the cloth. This is because the static friction between cloth and cup is sufficiently large enough. But when we slide the cloth with a very high speed, the cup will remain at its place and the cloth has moved out from beneath. The same principle is applied in the stick slip mechanism. The working principle for the stick slip actuators can be seen in figure 4.2. we can divide the movement in the following three steps. [41–43]

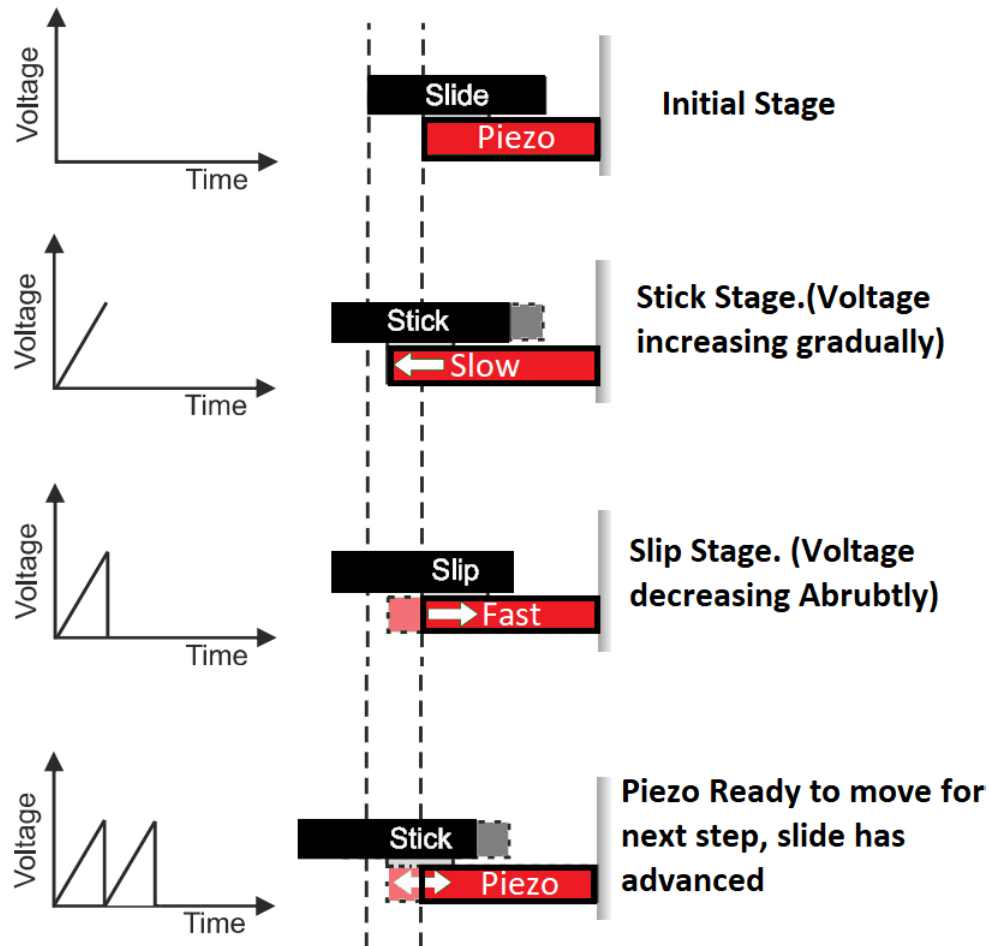


Figure 4.2: Stick Slip principle

1. **Initial state:** At the beginning the piezoelectric material is at its normal length and no voltage is applied at this stage.
2. **Stick State:** In this state the input voltage is increased gradually(0 100V). The length of piezoelectric material is increased gradually.Since the movement of piezoelectric material is significantly slow, the static friction between the slide and piezo electric material is sufficient enough that they stick to each other.The slide(end effector) which is placed on the piezo electric material now moves along with the piezoelectric material.

3. **Slip state:** In this state the input voltage is reduced abruptly. The piezoelectric material will contract back to its original length in very short time. Since the movement of piezoelectric material is very fast, the dynamic friction between the slide and piezo electric material is not sufficient to hold them together. Thus the slide slips on the piezo electric material and retain its extended position. However the piezoelectric material will return back to its initial stage [32]

If we desire to move the positioner backwards, than we can apply the same saw tooth voltage in reverse order such that the extension of piezoelectric material is done abruptly and the contraction is done slowly. The backwards movement of stick slip actuator can be seen in figure 4.3

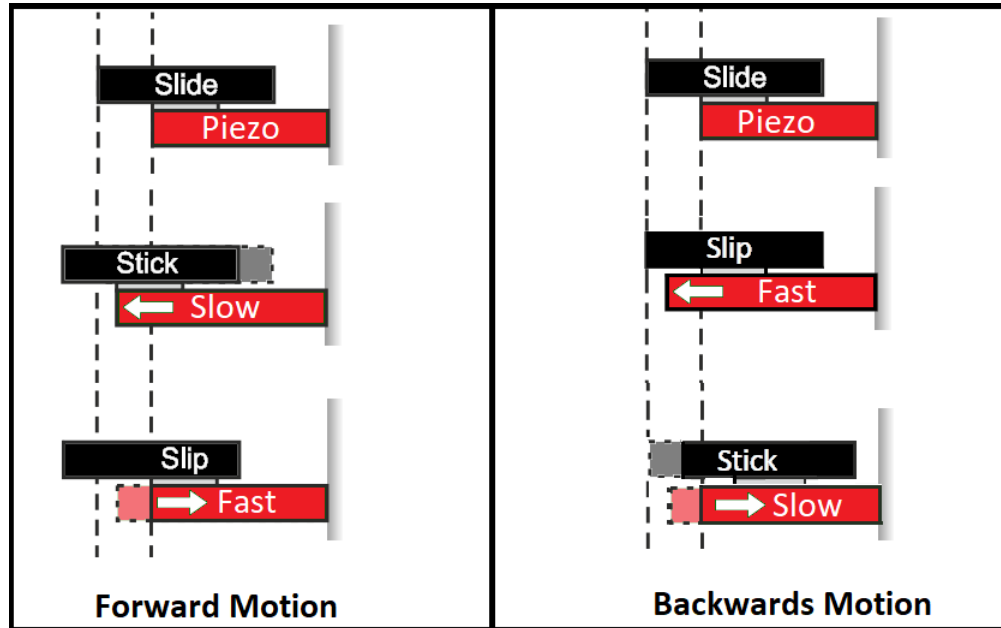


Figure 4.3: forward vs backward movement

4.3 Input Voltage Dynamics

SmarAct provides a DLL to control the stick slip piezoelectric actuator (SSPA) inside the labview environment. As discussed above, the positioner SLS-5282-L requires a repeating ramp signal as its input. In figure 4.4 a typical voltage signal is shown. To control the position of the end effector we can control some of the following parameters through labview.

1. **Number of Steps:** In this parameter we can specify how many number of steps of voltage that can be performed. Number of steps can be any integer value ranging approximately from $-10,000$ to $10,000$. Negative values indicate the motion of positioner in the backwards direction. Number of steps is directly proportional to the distance travelled by the end effector. The more the number of steps, the more distance will be travelled by the end effector.
2. **Voltage amplitude (V_{max}) :** The Peak voltage of the ramp signal is called the voltage amplitude or V_{max} . The range of the voltage amplitude is between 15Volts to 100 Volts however the unit of this parameter is 0.1 Volts so the actual range of Amplitude is 150(15V) to 1,000(100V). Voltage amplitude is directly proportional to the distance travelled by the end effector. By increasing the voltage amplitude we can increase the distance travelled per unit step.
3. **Frequency:** This parameter is the frequency (in Hz) that the steps are

generated with. we can also define the time period in seconds of the repeating ramp signal by using this parameter. the range of this parameter is from $5Hz$ to $18,500Hz$. The frequency is inversely proportional to the step width of the voltage signal. Increasing the frequency of the signal will decrease the step width of the voltage ramp signal. Changing the frequency will not change the distance travelled by the end effector in each step. it just changes the number of steps that can be executed in each second. Moreover the increase in frequency will result in alteration of the speed of motion of the end effector. A higher frequency will lead to a faster movement speed of the end effector.

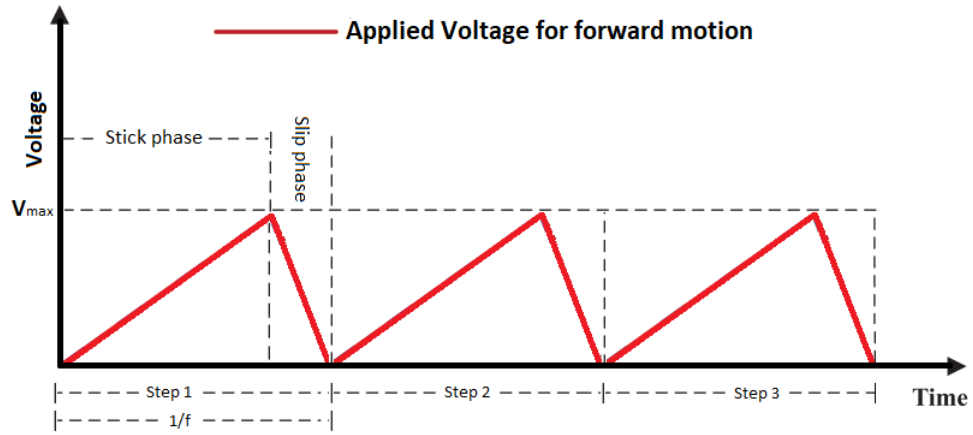


Figure 4.4: Input Voltage dynamics

4.4 General Control Scheme for Stick Slip Actuators

Since The Stick Slip Piezoelectric Actuators (SSPA) uses a ramp input voltage signal to operate as discussed above it is a challenging task to accurately control the movement. Proportional control is widely adopted to control the position of SSPA. In [18] a proportional control law is proposed for the position control of SSPA. The frequency of the ramp signal is directly proportional to the distance travelled. Thus the authors use frequency of the ramp signal to control the laser beam. In this study the authors neglected the friction and the hysteresis non linearity. In [2] a proportional control with voltage and frequency is presented. In [36] Authors presented a neural network based technique for the control of SSPA. Generally speaking a SSPA can be controlled in the following two stages.

1. **Single Step Control stage:** In this control stage, the actuator goes through one complete stick cycle and one complete slip cycle. Each stick and slip cycle movement is one step. By repeating multiple single steps we can reach closer to our desired position. Assume each step moves the positioner δ_{step} distance and the required length of movement is L_d then we need to repeat the single step control 'n' times to move the positioner at our required level. where we can find $n = \lfloor \frac{L_d}{\delta_{step}} \rfloor$. here $\lfloor x \rfloor$ is defined as the largest integer smaller than x. In single step control stage we are confined by the step size and the movement cannot be smaller than the δ_{step} . single

step control stage is used for course movement of the stages.

2. **Sub-step control phase:** After a coarse movement is done through single step control stage, the actuator is near its reference position. However we may require more accurate movement of the positioner. To include more precision we use the sub step control phase. In this state the end effector is moved with the desired precision towards the reference point. We could now carefully move the piezoelectric material with a very low acceleration such that it keeps on the stick stage and the end effector is moved along with it. In this case the accuracy of the end effector is the accuracy of the piezoelectric material itself. A possible drawback of this method is that the extreme slow speed of the end effector might not be desired in some cases. Another way is to allow the nonzero relative motion between the end-effector and the piezoelectric material. In this way, the relationship between the motion of the end-effector and the motion of the driving object should be modeled first. Then, the desired position of the driving object can be calculated by using this relationship and the predesigned reference of the end-effector. After that some advanced control methods of PEAs can be employed to drive the driving object to this desired position in a fast manner [35] [36].

A brief description of the single step control and sub step control stages are given in figure 4.5

SmarAct Provides us a labview literary through which we can modify and control the positioner SLS-5282-L. The control variables for this type of positioners

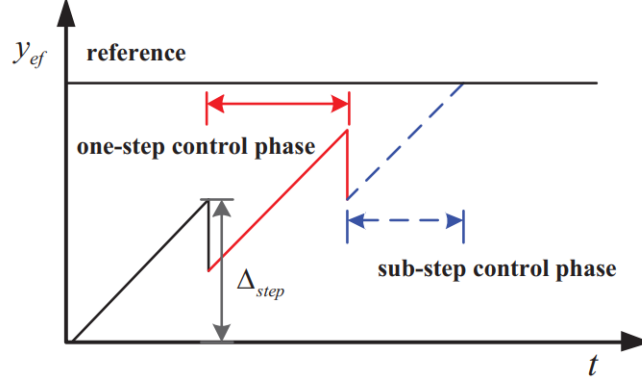


Figure 4.5: Single Step and sub step control

could be the frequency of input voltage, the amplitude of the voltage and the number of steps are described earlier.

4.5 Experimental Results: Proportional Control

In this section we will discuss the real time proportional feedback SLS-5282-L linear positioner. we have fixed the frequency and voltage amplitude and chosen to control the position of the positioner through steps as the feedback variable. The voltage amplifier/ controller that we are using to control the position is the SmarAct HCU-3CX controller. This Controller is a 3 channel controller with integrated sensor support. This controller allows us to measure the position of the end effector in the order of micrometers. We have fixed the Voltage amplitude to 1000(100V) and Frequency to 8000Hz. The Feedback variable is the steps applied. A proportional gain of 0.1 is applied. The Lab view Block Diagram for the proportional control is shown in figure 4.6

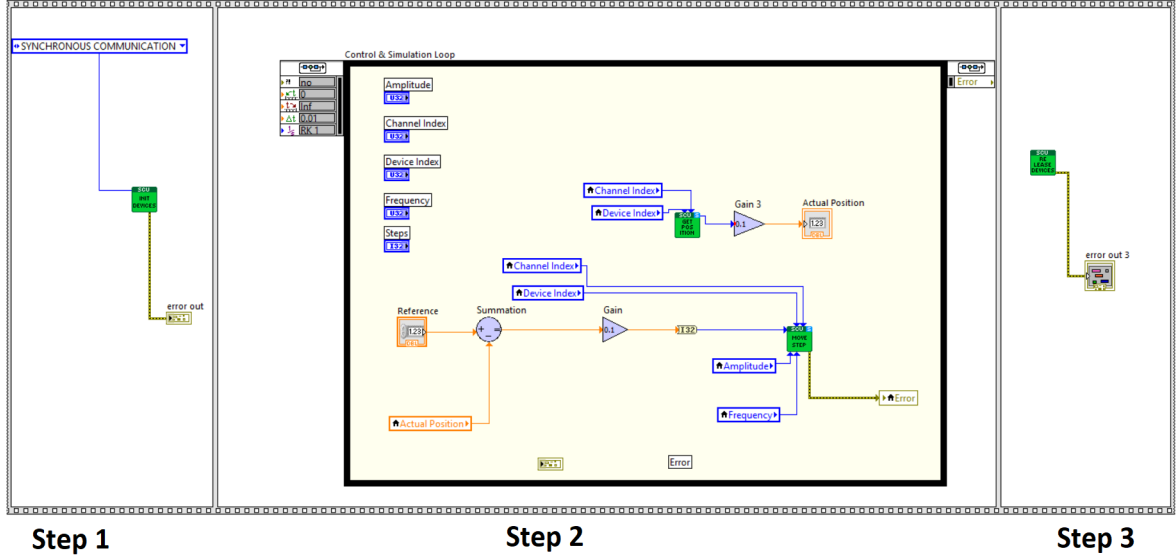


Figure 4.6: Labview Block Diagram for Proportional Control of SSPA

We have exported the data from labview control VI to an excel file and observed the behavior of the feedback control. A Reference of $5000 \mu\text{m}$ was given as a fixed value initially and we have applied the proportional control as shown in figure 4.6. We have used the integrated sensor to measure the position of the actuator.

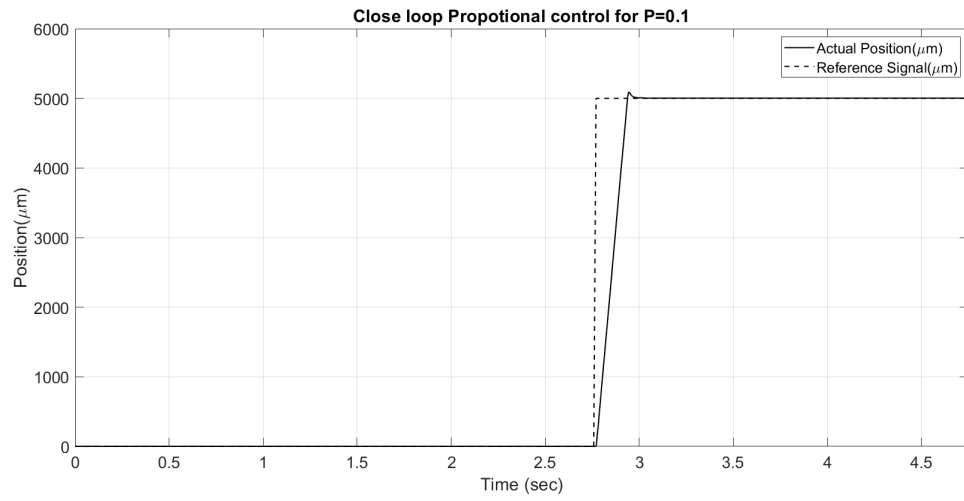


Figure 4.7: Proportional Control Output Plot (Position)

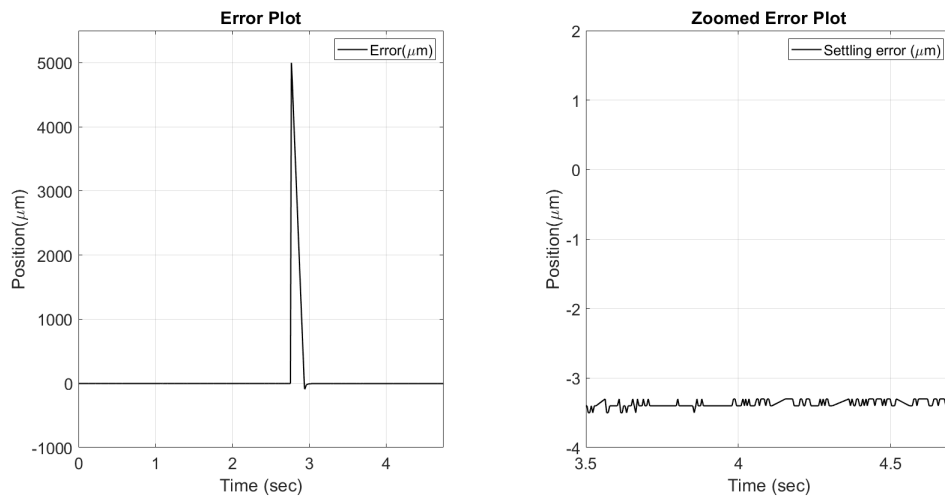


Figure 4.8: Proportional Control Error Plot

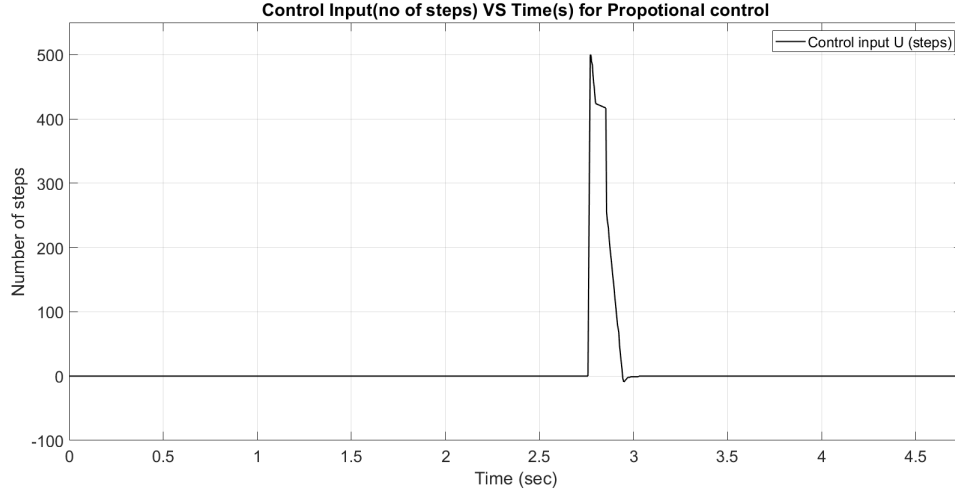


Figure 4.9: Proportional Control Input (number of steps applied)

In figure 4.7 the output position of the control loop is shown. Reference signal of $5000\mu m$ is applied at 2.75 seconds and the system settles down at around 3 seconds. From figure 4.7 it can be seen that the proportional feedback control is able to track the reference step signal with a sufficiently fast and accurate response.

Figure 4.8 we can observe the system error dynamics. initially the error is very large but the feedback forces the error to go back to near zero in approximately 0.25 seconds. In figure 4.8 part b, the error after settling down is shown. From this figure we can observe that the system error is settled around $-3.5\mu m$ so with the proportional control we observe a steady state error of around $-3.5\mu m$

Finally in figure 4.13 the control input U can be seen. We have converted the control input to its nearest integer value and we have a plot of number of steps

versus time. As expected initially a large number of steps is given as an input and after some time it reduces to zero as the error settles down.

4.6 Proportional Integral Control

In this section we will discuss the experimental result of the proportional integral control. We have fixed the Voltage amplitude to 1000(100V) and Frequency to 8000Hz. The Feedback variable is the number of steps. We have chosen a proportional gain of 0.1 and integral gain of 0.1 for this control. In Figure 4.10 the Block diagram for PI control in labview environment is shown.

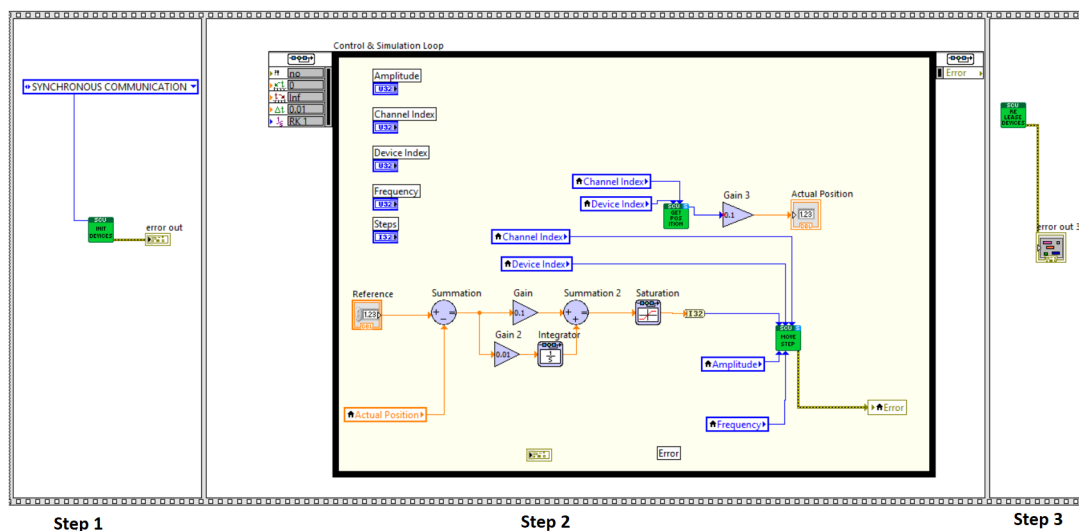


Figure 4.10: Labview Block Diagram for PI Control of SSPA

From figure 4.11 we can observe the step response for a proportional integral

feedback controller. The reference of $5000\mu m$ is applied at approximately 5.75 sec. we see a large overshoot as compared to the proportional controller and the settling time is also significantly larger. The system settles down at approximately 7.5 second.

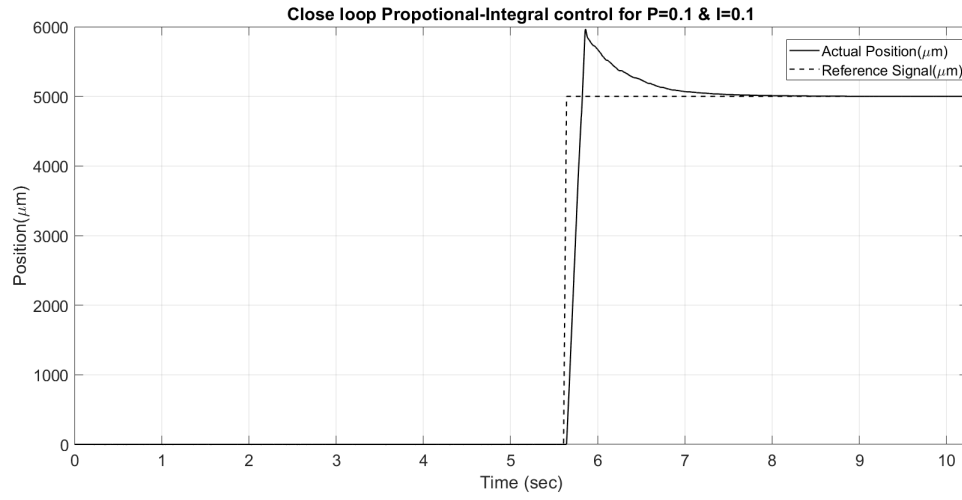


Figure 4.11: PI Control output plot(Position)t

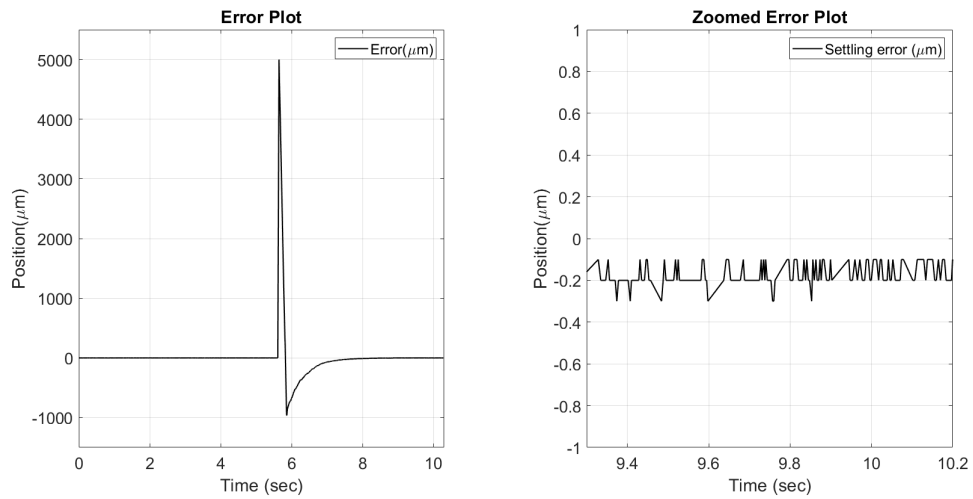


Figure 4.12: PI Error Plot

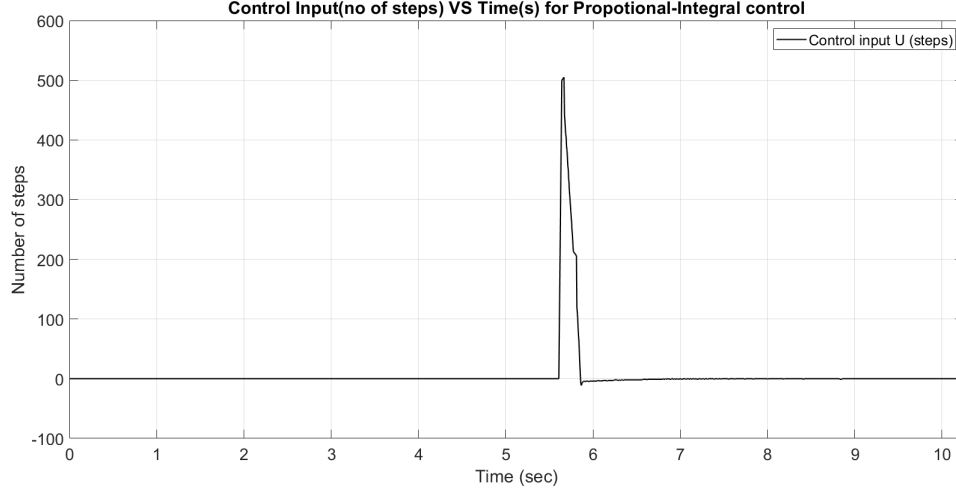


Figure 4.13: PI control Input plot (Number of steps applied)

The error plots for a PI controller can be seen in figure 4.12. From figure 4.12 part b we can observed a zoomed in view of the settling error. It can be seen that we have a steady state error of around $-0.2\mu m$. So a PI controller shows better steady state response as compared to the proportional controller.

The control input for the PI control (U) can be seen in figure 4.13. As expected , we observe a high value in the beginning, afterwards due to the PI control action we have an undershoot in control input to compensate for the overshoot in the position error. afterwards the control input settles down to zero.

4.7 System Identification

To apply model based control algorithms on the stick slip piezoactuator, the plant transfer function is required. Instead of analytical methods for system

identification a more practical way is to use the input and output information gathered from the open loop system. We can find the open loop system transfer function through LabView system identification tool box. We have used the input- output data gathered from the above experiment for proportional and proportional integral control and use this data to find out the approximate plant model. In figure 4.14 the results for system identification are shown for IO data acquired from Proportional control and in figure 4.15 the plant transfer function is calculated by using a PI control IO data. In figure 4.16 the labview code for system identification is shown. From the figure 4.14 the identified plant transfer function is found as follow 4.1

$$G_{identified}(s) = \frac{-0.040289s + 0.424381}{s - 0.0007613} \quad (4.1)$$

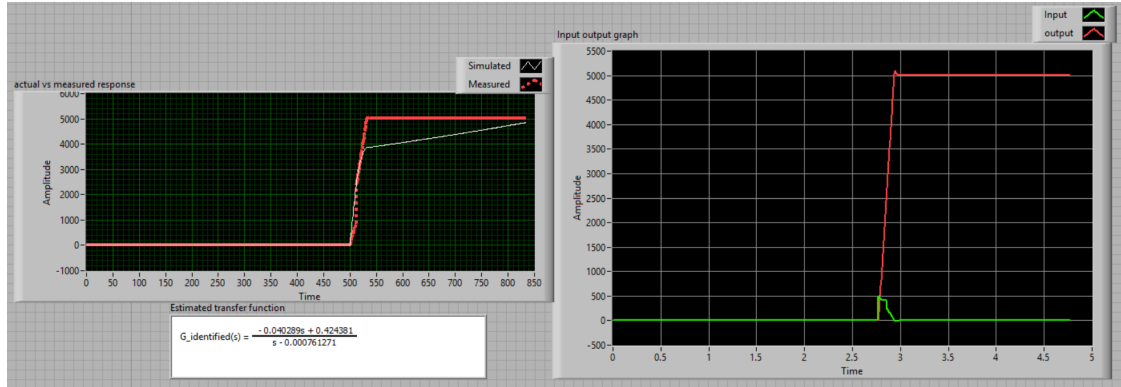


Figure 4.14: System identification by using IO data from proportional control

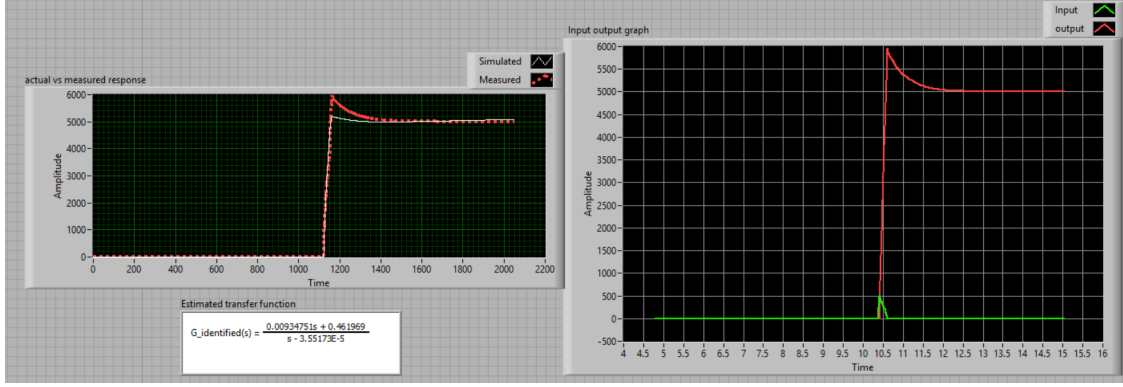


Figure 4.15: System identification by using IO data from PI control

Similarly we have used another data set obtained from the PI data set and approximates the identified plant model as a second order. The System model identification results are shown in figure 4.15. We can observe that although the identified plant has some error at the beginning but it converges to the end result. more data set might be used to increase the accuracy of the identify the plant model. The identified plant model for this data set is given as follow.

$$G_{identified}(s) = \frac{-0.0093s + 0.462}{s - 0.0000355} \quad (4.2)$$

The Identified plant might be used to apply more advanced algorithm like Iterative learning control e.t.c.

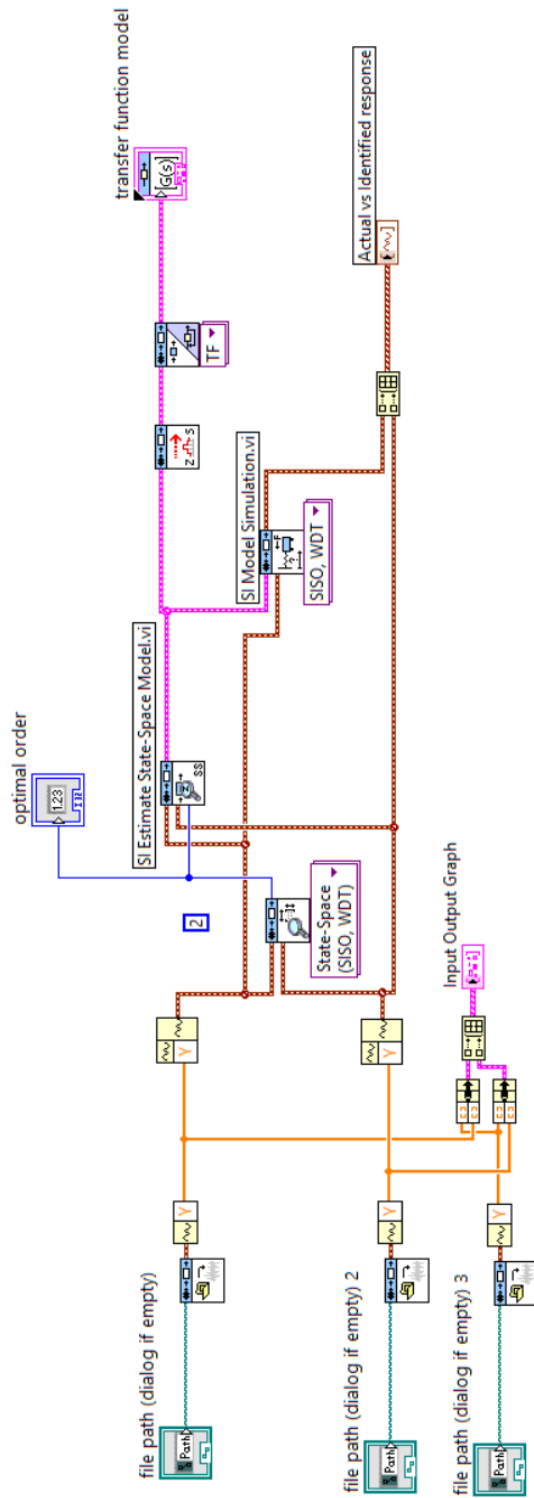


Figure 4.16: System identification Labview Block Diagram

CHAPTER 5

CONCLUSION AND FUTURE WORKS

Image processing is used as an initial alignment scheme for a laser beam steering experiment. In this experiment we have used a mini servo motor on which we have attached the laser beam transmitter. The steering mechanism is of angular type and the laser beam spot will move only in one dimension (vertical). The camera was able to detect the laser beam spot and drive the laser beam towards a fixed reference point which is marked as a blue spot. This color detection algorithm combined with a servo actuator enhances the dynamic movement range of the overall system. As compared to the PSD, camera provides a very large sensing area. The servo motor has a comparatively larger movement resolution as compared to the piezoactuators, thus the distance between the sensing area (Black Screen) and the laser beam transmitter must be kept as small as possible. Using a camera and servo motor is a cheap and effective solution of

the poor movement range of piezo actuators.

However Color detection algorithm also has its own limitations. For a reliable color detection we need a very good high color contrast between the back ground and the foreground. Since we are using a red laser beam spot, a black screen is a good alternative to the contrast problem. Lighting environment also plays a very important role in the color detection accuracy. A well lit and constant lighting environment is needed for this purpose.

Servo motor is a good choice due to its ease in control and motion, however a motor with an encoder will also provide us with better accuracy. Although the experiment provides sufficiently better results , Using single motor will only result in one directional control. To steer the beam in the second dimension we might need to couple the laser beam with a second motor.

A Proportional (P) and Proportional Integral (PI) controller is implemented on a stick slip actuated piezoactuator. A labview program is used to acquire the data and implement the control law. The Proportional controller provides a better transient behavior with fast response, very small overshoot and fast settling time. In proportional control we observe a relatively higher steady state error of $-3.5\mu m$. On the other hand the PI controller shows relatively poor transient behavior with slow response , a high overshoot , and slow settling time . But the steady state response of PI controller is far superior than that of Proportional controller with a settling error of $-0.2\mu m$.

Although PI controller can be used for vary high accuracy of $0.2 \mu m$, the large overshoot problem of PI controller needs improvements. Moreover in this study we have observed the control for one dimensional system only. We might want to extend the results to a 2 dimensional system by combining two SSPAs. In this study we have fixed the Step size, voltage amplitude and frequency given to the SSPA. Thus we have controlled the system with a single step control only. Since the available controller does not offer us to control the system with sub step control, we may investigate the results further by reducing the step size.

APPENDIX A

EQUIPMENT LIST

Sr.No	Model No	Brief Description
1	<i>HNLS008L</i>	Laser Source
2	<i>K1PZ</i>	3-Axis Piezo actuator
3	<i>MDT694B</i>	ThorLabs Piezo Mirror Actuator
4	<i>KPA101</i>	Beam Position Aligner
5	<i>PDQ80A</i>	Position sensing detector
6	<i>BFS20 – A</i>	Beam Splitter
7	<i>STT – 25.4 – CE – I</i>	SmarAct Piezo Mirror Actuator
8	<i>eton5949</i>	USB Camera

Table A.1: Main parts used in the experiment

APPENDIX B

PSD PIN DIAGRAM

PIN	Description
1	X-axis $[Q2 + Q3] - [Q1 + Q4]$
2	Y-axis $[Q1 + Q2] - [Q3 + Q4]$
3	SUM $[Q1 + Q2 + Q3 + Q4]$
4	+5 V to +15 V
5	Common
6	-5 V to - 15 V

Table B.1: Pin Diagram of PDQ80A Position Sensor

APPENDIX C

DATE SHEETS

OPTO-MECHANICS

STT-25.4-CE

Close-Loop Motorized Optical Mount in Clear Edge



< 0.1 μ rad



$\Phi, \Theta: \pm 2.5^\circ$



available



down to
 10^{-11} mbar

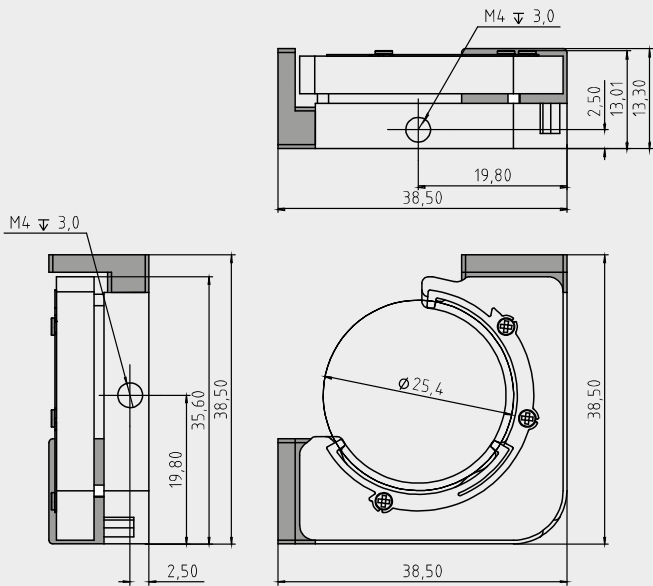


35.6 x 35.6 x
12.3 mm³

Mechanical Properties	
mirror mount	25.4 mm (1 ")
range Θ^*	$\pm 2.5^\circ$
range Φ^*	$\pm 2.5^\circ$
thread for optical mount	M4
positioner dimension	38.5 x 38.5 x 13.3 mm ³
weight	25 g
Positioning	
step width	2 μ rad to 40 μ rad
scan range	40 μ rad
scan resolution	< 0.1 μ rad
speed**	$\approx 15^\circ/\text{s}$
max. frequency	18.5 kHz
Materials and Vacuum Options	
black anodized (-BK)	
closed-loop on request only	
non magnetic materials (-NM)	
-HV (10^{-6} mbar), -UHV / -UHVt (10^{-11} mbar)	



Close Loop with inductive Sensor (-I)	
sensor resolution	$1.4 \cdot 10^{-3}^\circ$
accuracy	$\pm 0.02^\circ$
bidirectional position repeatability	0.01°



Grey parts mark the optional position sensor. Linear dimensions are given in mm.

* For close loop mirror mount $\pm 2.15^\circ$
** For close loop mirror mount $9^\circ/\text{s}$

LINEAR POSITIONERS

SLC-1780

Nanometer Precision Linear Positioner



< 1 nm



51 mm



30 N (3 kg)



available

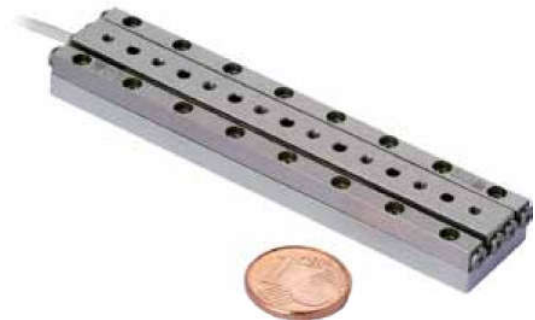


down to
10⁻¹¹ mbar

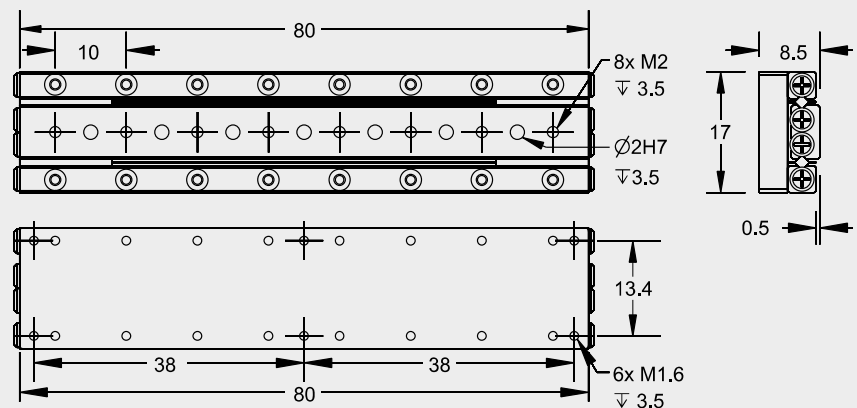


80 x 17 x 8.5
mm³

Mechanical Properties	
blocking force F_B	> 3.5 N
max. normal force F_N	30 N
max. lift force F_L	> 1.5 N
positioner dimension	80 x 17 x 8.5 mm ³
weight	51 g
pitch torque M_p	12.5 Nm
yaw torque M_y	12.5 Nm
roll torque M_R	1.9 Nm
Positioning	
travel	± 25.5 (51) mm
step width	1 - 1,500 nm*
scan range	> 1.5 µm
scan resolution	< 1 nm
velocity	> 20 mm/s
max. frequency	18.5 kHz
Materials and Vacuum Options****	
steel base (-ST), titanium base (-TI)	
non magnetic materials (-NM*****)	
black anodized (-BK)	
integrated connecting elements (-O)	
external support for increased M_y , M_R (-W)	
high precision bearing (-P)	
increased blocking force (-D, +1.5 N)	
-HV (10 ⁻⁶ mbar), -UHV / -UHVT (10 ⁻¹¹ mbar)	



Closed-Loop with -S	
sensor resolution	1 nm
repeatability	± 80 nm**
Closed-Loop with -L***	
sensor resolution	4 nm
closed loop resolution	± 500 nm (H)CU 4 nm MCS
repeatability	± 1 µm (H)CU ± 160 nm MCS
Closed-Loop with -M***	
sensor resolution	100 nm
closed loop resolution	500 nm (H)CU 100 nm MCS
repeatability	± 2.5 µm (H)CU ± 0.5 µm MCS



Linear dimensions are given in mm.

CONTROL SYSTEMS

MODULAR CONTROL SYSTEM

Scalable Micro- and Nanopositioning Control

The Modular Control System (MCS) is suitable for both micro- and nanopositioning tasks.

Thanks to the modular concept we can assemble control systems with the number of channels matching the connected positioning systems. Accordingly, you can combine multiple driver modules and control them via the same computer-interface.

Attaching a sensor-module allows you to control our positioners in closed-loop mode.

It can connect up to three positioners to one driver module and is available for the three sensor-types -S, -L and -M.

The MCS is also available as a 19"-rack mount chassis-module or as a naked board for OEM products.

Three different computer interfaces are available: USB, Ethernet and RS-232.

In case of USB and Ethernet, we deliver the controller

with Windows DLL, LabVIEW driver and simple control program.

If you prefer ASCII commands, you can choose between Ethernet- or RS-232-interface.

Furthermore, you can control connected positioning systems manually when adding a hand-controller module to the MCS.



MCS-3CC-3H-USB-TAB

MCS three channel control system with integrated hand-control module for manual positioning.

DRIVER MODULES

Each MCS controller contains driver modules and / or end effector modules to control different positioners and/or end-effectors.

Each driver module can control up to three positioners. Therefore, MCS controllers with three, six, nine, etc. control channels are available. A driver module creates the necessary signals for driving the connected positioners in step- and scan-mode. Additionally, the driver module processes and controls the measured position (closed-loop control) when a closed-loop positioner is connected via a sensor-module.



MCS-3S-EP-SDS15-TAB

MCS sensor module for a three channel control system.

SENSOR MODULES

If you want to use closed-loop positioners with integrated nano- or microposition sensors an external sensor-module is necessary which digitizes the sensor data. The MCS driver module calculates and controls the current position based on the sensor signals. There are many different sensor-module options available:

- MCS-nM/L/S-.. for n positioners with integrated -M, -L or -S sensor
- MCS-...-TAB for table top housing (see image below)
- MCS-...-LEMO for housing with Lemo connectors
- MCS-...-OEM for integration into system baseplates

Self-Contained HeNe Laser: 0.8 mW, Polarized, 120 VAC

HNLS008L



Description

Thorlabs' cylindrical, low-power, red (632.8 nm) Helium-Neon lasers are available with output powers from 0.8 to 2.0 mW. Thorlabs offers these 632.8 nm lasers with either linear (>500:1) or random polarization and beam divergences ranging from 1.3 to 1.7 mrad.

Specifications

General	
Wavelength	632.8 nm
Minimum Output Power (TEM ₀₀)	0.8 mW
Minimum Polarization Ratio	500:1
Beam Diameter (TEM ₀₀ , 1/e ² points + 3%)	0.48 mm
Beam Divergence (TEM ₀₀ , +3%)	1.7 mrad
Mode Purity (TEM ₀₀)	>95%
Longitudinal Mode Spacing	1090 MHz
Maximum Noise (RMS) (30 Hz to 10 MHz)	1.0%
Maximum Drift*	± 2.5%
Maximum Mode Sweeping Contribution	10%
Operating Voltage (± 100 V)	1250
Operating Current (± 0.1 mA)	4 mA
Maximum Starting Voltage	10 kV DC

*With respect to mean power over 8 hours.

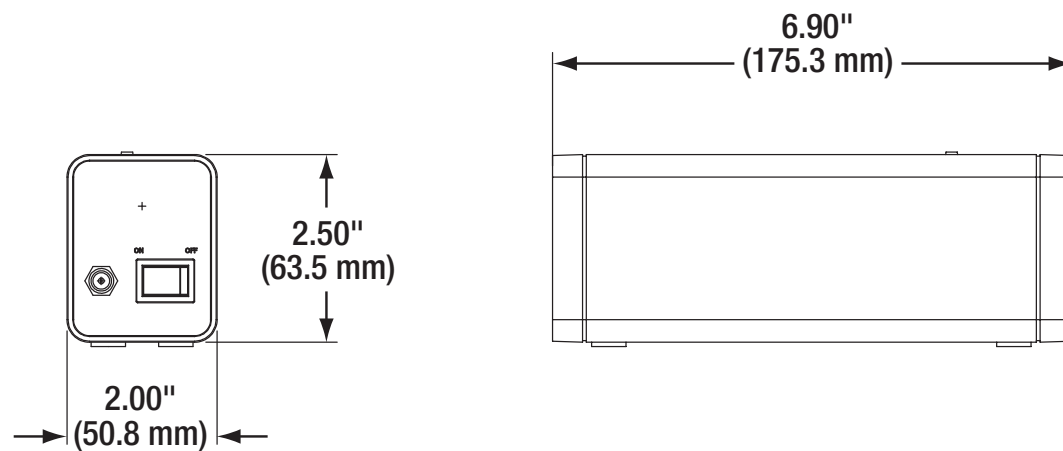
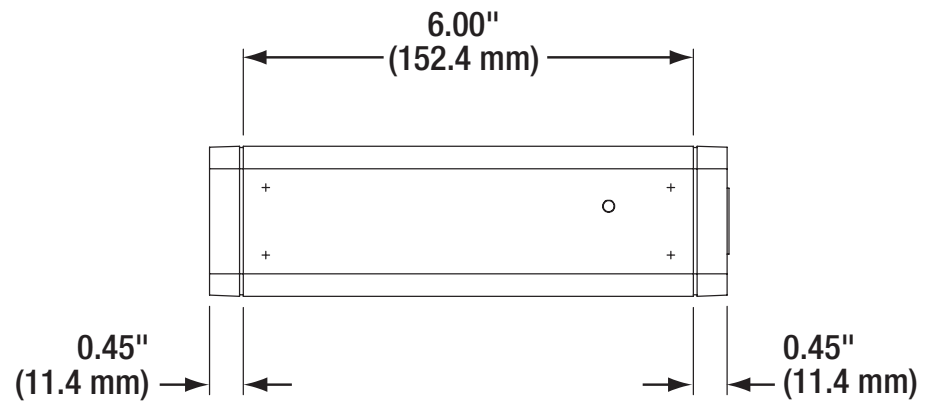
Physical / Mechanical	
Maximum Warm-Up Time (95% Power)	10 min
Storage Lifetime	Indefinite (Hard-Sealed)
Static Alignment	Approximately 1.75" from Base
Laser Weight	1.1 lbs (0.5 kg)

Environmental	
Operating Temperature	-40 to 60 °C
Non-Operating Temperature	-40 to 100 °C
Operating Altitude	0 to 10,000 ft
Non-Operating Altitude	0 to 70,000 ft
Relative Humidity (Non-condensing)	Non-Condensing
Shock	25 g for 11 ms 100 g for 1 ms

Safety	
CDRH/IEC 60825-1 Class	IIIa/3R



Drawings



PDQ80A



Description

The PDQ80A detector is a segmented, position sensing, silicon, quadrant detector for precise path alignment of light in the 400 to 1050 nm range. The device is capable of measuring beams with a spot size smaller than 7.8 mm, which is the diameter of the quadrant photodiode array. To prevent beam walk-off however, it is recommended that the beam diameter be less than 3.9 mm. Also, since the detected signal strength decreases significantly when large portions of the spot cross the boundary between the quadrants, beam diameters greater than 1 mm are suggested. Therefore, it is recommended that this device be used with beams with a diameter between 1 mm and 3.9 mm.

Specifications

Electrical Specification	
Vavelength Range	400 - 1050 nm
Peak Responsivity :	
(633 nm)	0.4 A/W
(900 nm)	0.64 A/W
Transimpedance gain	10 kV/A
Max Photocurrent	200 μ A
Output Voltage Range	± 2 V _{min}
Signal Output Offset	100 mV _{max}
Bandwidth	150 kHz
Recommended Spot Size	$\varnothing 1.0$ - 3.9 mm
Supply Voltage Requirement	± 5 VDC $\pm 5\%$, 35 mA
Operating Temperature	10 to 40 $^{\circ}$ C
Storage Temperature	-20 to 80 $^{\circ}$ C

Physical Specifications	
Sensor Size	$\varnothing 7.8$ mm
Clear Aperture	$\varnothing 1/2"$ ($\varnothing 12.7$ mm)
Aperture Thread	SM05 (0.535" -40)
Dimensions	2.00" x 1.20" x 0.65" (50.8 x 30.5 x 16.5 mm)
Mounting Thread	8-32 x 0.25" min depth
Metric Adapter	M4 to 8-32 Adapter (Item 3 AS4M8E)
Cable Length	5.0' (1.5m)
Connector (Plug)	Hirose HS10A-7P-6P
Main Receptacle	Hirose HR10A-7R-6S
Weight	0.25 lbs (114 g)

Instructions

1. Unpack the PDQ80A sensor, and install the adapter if metric mounting is preferred.
2. Plug the connector into one port of a PDQ80S1 hub.
3. Follow the directions for operation of the hub as described in its operating manual.
4. Place a spot onto the detection window for measurement. The input beam spot size should be between $\varnothing 0.2$ mm and $\varnothing 7$ mm. For best results the spot should be located within 80% (7.2 mm x 7.2 mm) of the center of the detector. Adjust the power level so that the SUM output voltage is less than or equal to 4 V. This will ensure the best signal to noise ration and that the system is not saturated.



Application Note

For best results low power levels should be used for the position sensor. For the PDQ80A the max photocurrent is 2 V / 10 kV/A = 200 μ A. Using the photosensitivity curve below, the system saturation power can be calculated as:

$$P_{max} = \frac{200 \mu A}{\text{Photosensitivity (A/W)}}$$

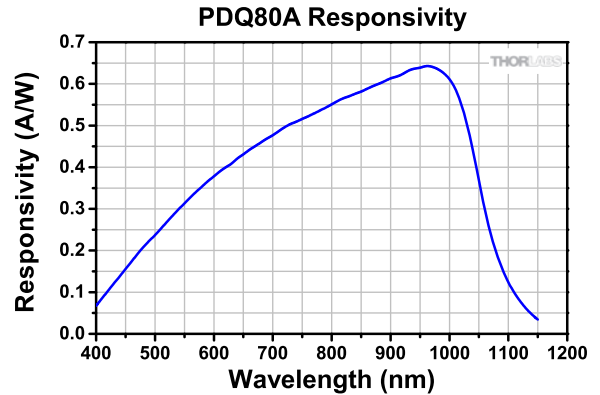
The PDQ80S1 hub has a sample resolution of 12 bits with an input voltage range of ± 5 V (10 V range), or a voltage resolution of:

$$V_{step} = \frac{10 \text{ V}}{2^{12}} = 2.44 \text{ mV}$$

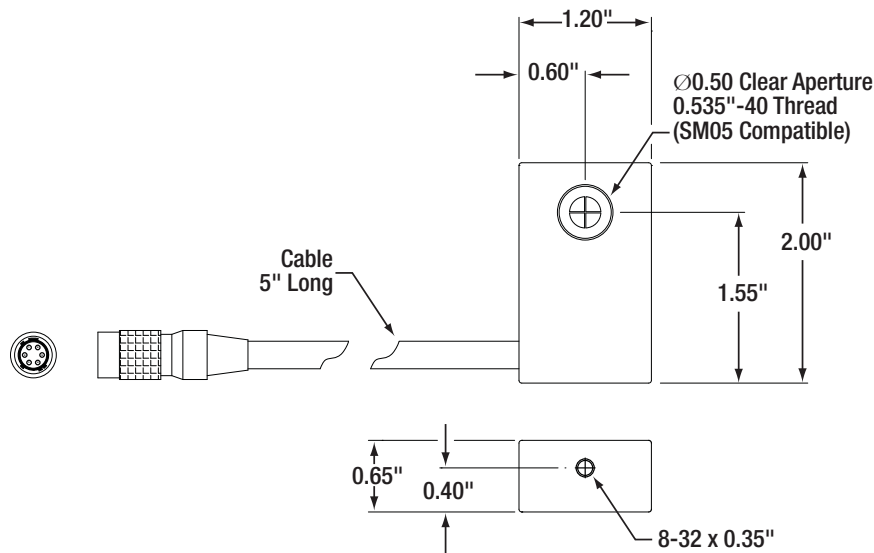
$$I_{step} = \frac{V_{step}}{10 \text{ kV/A}} = 244 \text{ nA}$$

From this the minimum power required can be determined based on the required accuracy. For example if the user requires an accuracy of 1% then the reading must be accurate to 1 part in 100. The minimum photocurrent is therefore the $I_{step} \times 100$, or $24.4 \mu A$. Use the Formula below to find the minimum optical power for a given wavelength.

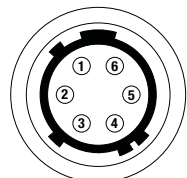
$$P_{min} = \frac{24.4 \mu A}{\text{Photosensitivity (A/W)}}$$



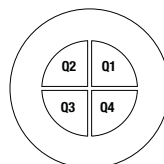
Drawings



Pin Assignments	
PIN 1	X-Axis (Q2 + Q3) - (Q1 + Q4)
PIN 2	Y-Axis (Q1 + Q2) - (Q3 + Q4)
PIN 3	SUM (Q1 + Q2 + Q3 + Q4)
PIN 4	+V (+5 V to +15 V)
PIN 5	COMMON
PIN 6	-V (-5 to -15 V)



HIROSE CONNECTOR



PHOTODIODE DETAIL

POLARIS-K1PZ Mirror Sold Separately



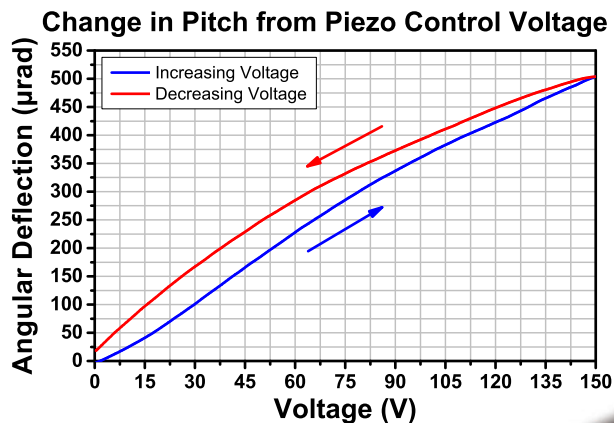
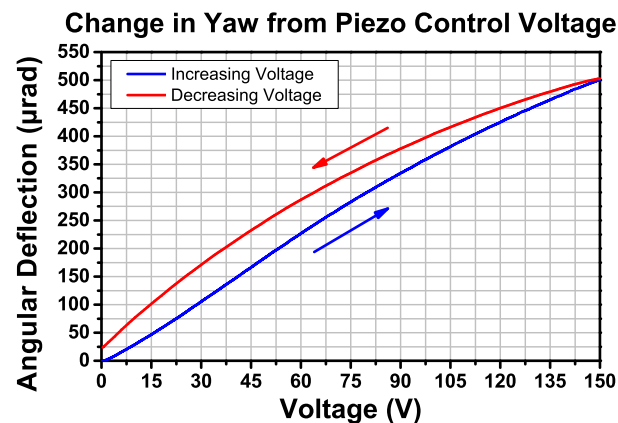
Specifications

POLARIS-K1PZ	
Optic Specifications	
Optic Size	Ø1" (Ø25.4 mm)
Optic Thickness (Min)	0.08" (2 mm)
Optic Mounting Torque	6 to 10 oz-in for 6 mm Thick Optics (Recommended)
Beam Deviation after Temperature Cycling ^a	<3 µrad
Adjuster Specifications	
Angular Range	Mechanical: ±5° Piezo: >500 µrad
Angular Resolution	Mechanical: ~7 mrad/rev Piezo: ~0.5 µrad for a 0.1 V Step ^b
Adjusters	Manually Adjustable 100 TPI Screws with Integrated Piezoelectric Elements and Matched Actuator/Body Pairs (3 Screws Total)
Piezo Control Voltage	0 to 150 V
Piezo Connectors	Male SMB (Three SMB-to-BNC Cables Included)
Physical Specifications	
Mounting	Two #8 (M4) Counterbores at 90°
Vacuum Compatibility	10 ⁻⁵ Torr at 20 °C Epoxy Meets Low Outgassing Standards NASA ASTM E595, Telcordia GR-1221
Operating Temperature	-25 to 85 °C



- While the POLARIS-K1PZ was physically disconnected from its piezo controller (zero bias), the ambient temperature was increased by 15 °C, then allowed to return to room temperature.
- Measured by incrementing and decrementing the voltage applied by a TPZ001 controller in 0.1 V steps.

Hysteresis Curves



Optic Installation

Ensure that there is no grease, dirt, or dust in the optic bore or on the optic itself.

Remove any particulates with compressed air and/or clean with acetone or methanol. With the mount oriented at $\sim 45^\circ$ so that it stands on its corner adjuster, place the optic into the bore.

Lightly tap the edge of the faceplate with the plastic handle of a balldriver. This will adjust the optic's position so that it makes the correct contact with the two contact lines and the locating lip. Finally, use a ball driver or hex key to engage the optic retaining screw, preferably to the specific torque.

Since the mirror expands at a different rate than the mounting mechanism, it is essential to hold the optic firmly in place. A torque of 6 to 10 oz-in (0.375 to 0.675 lb-in; 0.04 to 0.07 N•m) applied to the optic's mounting setscrew produces optimal results for a 6 mm thick mirror (use Thorlabs' TD24 Torque Wrench). Furthermore, when tightening the Polaris mount to a $\varnothing 1$ " post, a torque of 14 to 16 lb-in (1.6 to 1.8 N•m) is optimal and minimizes the mount's slippage due to temperature changes (use Thorlabs' TD75 Torque Wrench).

Usage Tips

General Usage Tips

- 1) **Match Materials:** Due to its relatively low coefficient of thermal expansion, 303 stainless steel was chosen as the material from which to fabricate the Polaris mount. When mounting the POLARIS-K1PZ, we recommend using components fabricated from the same material.
- 2) **Use a Wide Post:** The Polaris' performance is optimized for use with a $\varnothing 1$ " RS series post. These posts provide two planes of contact with the mount, which help confine the bottom of the mount during variations in the surrounding temperature, thereby minimizing potential alignment issues.
- 3) **Mount an Optic only when the Mount is out of a Setup:** Since an optic is prone to movement within its mounting bore, all optics should be mounted with the Polaris out of the setup to ensure accurate mounting that will minimize misalignment effects.
- 4) **Front Plate's Position:** To achieve the best performance, it is recommended that the front plate be kept as parallel as possible to the back plate. This ensures the highest stability of the adjustments.
- 5) **Mount as Close to the Table's Surface as Possible:** To minimize the impact of vibrations and temperature changes, it is recommended that your setup have as low of a profile as possible. Using short posts will reduce the Y-axis translation caused by temperature variations and will minimize any movements caused by vibrations.
- 6) **Polish and Clean the Points of Contact:** We strongly recommend that the points of contact between the mount and the post, as well as the post and the table, are clean and free of scratches or defects. For best results, we recommend using a polishing stone to clean the table's surface and a polishing pad (Thorlabs Item # LFG1P) for the top and bottom of the post as well as the bottom of the mount.

Piezo Usage Tips

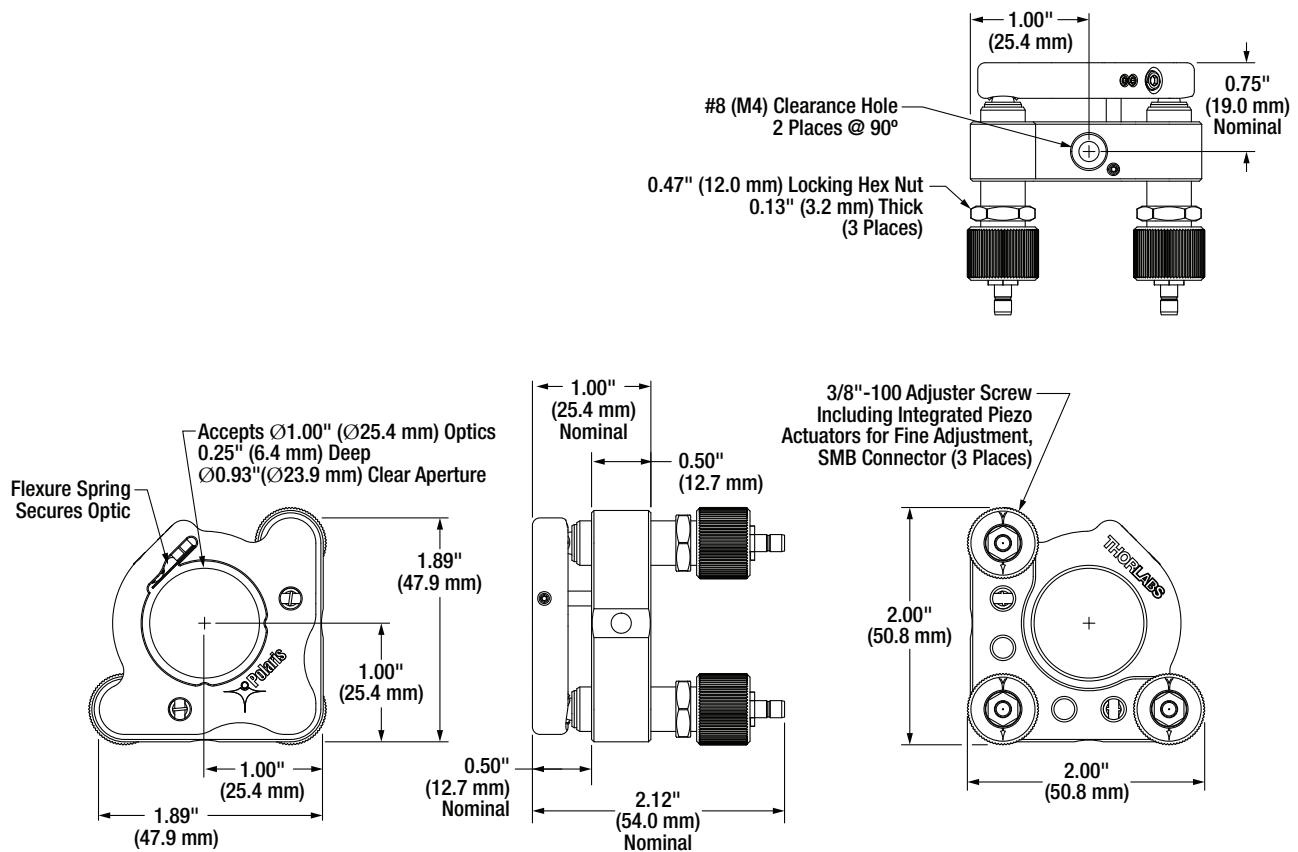
- 1) **Mount on a Ceramic Pedestal Post:** Thorlabs' $\varnothing 1$ " pillar posts can be secured to a ceramic pedestal post (Thorlabs Item # RS05PC) for increased thermal and electrical isolation. The glass-mica ceramic insulates the Polaris mount from the optical table or breadboard, preventing potential electrical loops from forming that can increase the noise seen by the piezo connector and lead to beam drift.
- 2) **Disconnect Unused Channels:** If active stabilization of a given axis is not needed, then it is not necessary to connect the unused axis to a piezoelectric controller. Any noise on the electrical connection may cause an undesired movement in the beam.

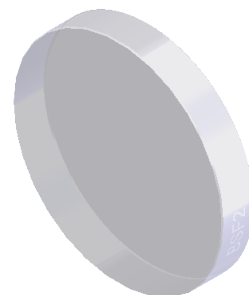
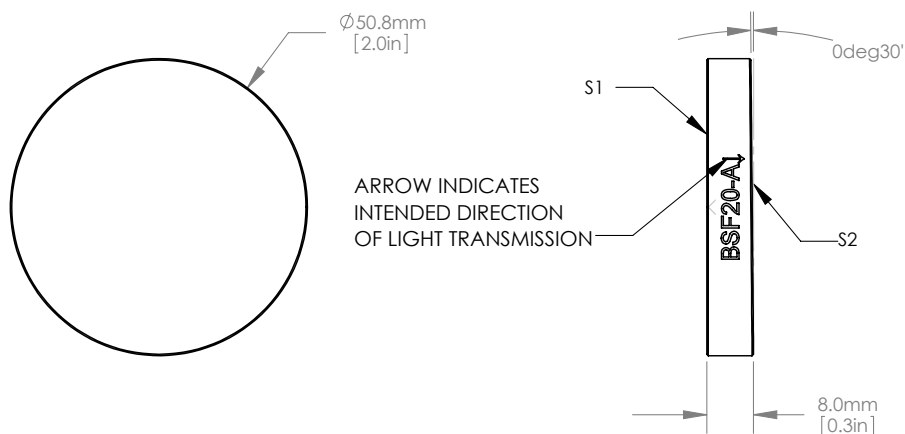
- 3) **Connect Cables only when Power Supply is Off:** The piezoelectric stacks may be irreversibly damaged by abrupt changes in the applied voltage. In order to prevent such damage, ensure that the power supply is off before connecting the SMB cable.
- 4) **Use Gentle Voltage Steps:** Abrupt charging or discharging of the piezoelectric actuator may cause irreversible damage to the piezo.
- 5) **Stay within the 0 - 150 V Control Voltage Range:** Applying voltages less than 0 V (negative voltages) or greater than 150 V may cause irreversible damage to the piezo.
- 6) **Handle with Care:** Piezoelectrics are ceramic materials, and therefore relatively brittle as compared to common optomechanics. Hence, they are sensitive to shock forces. Do not drop the mount or place it in a box without protective cushioning.

Not Recommended

- Do not take the adjusters out of the body as it can cause the threading to be contaminated, greatly reducing the mount's fine adjustment performance.
- Do not pull the front plate away as it might stretch the springs beyond their operating range, crack the sapphire seats, or break the piezoelectric stacks.

Drawings






NOTES/SPECIFICATIONS:

1. CLEAR APERTURE: >45.72mm
2. SURFACE FLATNESS(S1, S2): $\lambda/8$ AT 633nm OVER CLEAR APERTURE
3. SURFACE QUALITY (S1, S2): 20-10 SCRATCH-DIG
4. THICKNESS TOLERANCE: ± 0.40 mm
5. DIAMETER TOLERANCE: $+ 0.00/-0.20$ mm
6. WEDGE TOLERANCE: ± 10 arcmin
7. COATING (S1): NONE
8. COATING (S2): BBAR 350nm-700nm
Ravg: < 1.0%
AOI: 45°

FOR INFORMATION ONLY
NOT FOR MANUFACTURING PURPOSES

DRAWING PROJECTION			THORLABS www.thorlabs.com	
	NAME	DATE	Ø2" BEAM SAMPLER, A COATING	
DRAWN	GG	18/MAY/12		
APPROVAL	DD	08/JUNE/17	MATERIAL	
COPYRIGHT © 2017 BY THORLABS			UV FUSED SILICA	
VALUES IN PARENTHESIS ARE CALCULATED AND MAY CONTAIN ROUND OFF ERRORS			ITEM #	APPROX WEIGHT
			BSF20-A	36 g

REFERENCES

- [1] S. Muta, T. Tsujimura, and K. Izumi, “Laser beam tracking system for active free-space optical communication,” in *Proceedings of the 2013 IEEE/SICE International Symposium on System Integration*, Dec 2013, pp. 879–884.
- [2] M. Rakotondrabe, Y. Haddab, and P. Lutz, “Voltage/frequency proportional control of stick-slip micropositioning systems,” *IEEE Transactions on Control Systems Technology*, vol. 16, no. 6, pp. 1316–1322, Nov 2008.
- [3] T. Tsujimura, S. Muta, Y. Masaki, and K. Izumi, “Initial alignment scheme and tracking control technique of free space optics laser beam,” in *2014 5th International Conference on Optical Communication Systems (OPTICS)*, Aug 2014, pp. 1–6.
- [4] H. Yoon, B. E. Bateman, and B. N. Agrawal, “Laser beam jitter control using recursive-least-squares adaptive filters,” *Journal of Dynamic Systems, Measurement, and Control*, vol. 133, no. 8, pp. 041 001–1, 2011.
- [5] W. Zhu, L. Bian, Y. An, G. Chen, and X. Rui, “Modeling and control of a two-axis fast steering mirror with piezoelectric stack actuators for laser beam

- tracking,” *Smart Materials and Structures*, vol. 24, no. 7, p. 075014, 2015.
- [6] N. O. Perez-Arancibia, J. S. Gibson, and T. C. Tsao, “Observer-based intensity-feedback control for laser beam pointing and tracking,” *IEEE Transactions on Control Systems Technology*, vol. 20, no. 1, pp. 31–47, Jan 2012.
- [7] C. Wei, C. Sihai, W. Xin, and L. Dong, “A new two-dimensional fast steering mirror based on piezoelectric actuators,” in *2014 4th IEEE International Conference on Information Science and Technology*, April 2014, pp. 308–311.
- [8] J. Wang and J. M. Kahn, “Acquisition in short-range free-space optical communication,” pp. 4873 – 4873 – 12, 2002.
- [9] H. Willebrand and B. S. Ghuman, *Free space optics : enabling optical connectivity in today’s networks*. Indianapolis, Ind. : SAMS, 2002.
- [10] J. P. Dodley, D. M. Britz, D. J. Bowen, and C. W. Lundgren, “Free-space optical technology and distribution architecture for broadband metro and local services,” 2001.
- [11] S. Grafstrm, U. Harbarth, J. Kowalski, R. Neumann, and S. Noehte, “Fast laser beam position control with submicroradian precision,” *Optics Communications*, vol. 65, no. 2, pp. 121 – 126, 1988.
- [12] A. Malik and P. Singh, “Free space optics: Current applications and future challenges,” in *International Journal of Optics*, vol. 2015, 2015, p. 7.

- [13] A. Mansour, R. Mesleh, and M. Abaza, “New challenges in wireless and free space optical communications,” vol. 89, no. Supplement C, 2017.
- [14] H. Kaushal and G. Kaddoum, “Free space optical communication: Challenges and mitigation techniques,” *CoRR*, vol. abs/1506.04836, 2015.
- [15] H. Henniger and O. Wilfert, “An introduction to free-space optical communications,” 2010.
- [16] S. Devasia, E. Eleftheriou, and S. O. R. Moheimani, “A survey of control issues in nanopositioning,” *IEEE Transactions on Control Systems Technology*, vol. 15, no. 5, pp. 802–823, Sep. 2007.
- [17] Y. Tashiro, Y. Suito, K. Izumi, K. Yoshida, and T. Tsujimura, “Optical system design for laser tracking of free space optics,” in *2017 56th Annual Conference of the Society of Instrument and Control Engineers of Japan (SICE)*, Sept 2017, pp. 1098–1103.
- [18] J. . Breguet and R. Clavel, “Stick and slip actuators: design, control, performances and applications,” in *MHA’98. Proceedings of the 1998 International Symposium on Micromechatronics and Human Science. - Creation of New Industry - (Cat. No.98TH8388)*, Nov 1998, pp. 89–95.
- [19] G. Gu, L. Zhu, C. Su, H. Ding, and S. Fatikow, “Modeling and control of piezo-actuated nanopositioning stages: A survey,” *IEEE Transactions on Automation Science and Engineering*, vol. 13, no. 1, pp. 313–332, Jan 2016.

- [20] J.-Y. Yen, C.-S. Jeng, and K.-C. Fan, “Servo design for a 3-d lasertracking measurement system,” *Transactions of the ASME Journal of Dynamic Systems, Measurement, and Control*, vol. 118, no. 3, pp. 476–481, September 1996.
- [21] M. Hernandez-Gonzalez and M. A. Jimenez-Lizarraga, “Real-time laser beam stabilization by sliding mode controllers,” *The International Journal of Advanced Manufacturing Technology*, vol. 91, no. 9, pp. 3233–3242, Aug 2017.
- [22] X. Wanga, C. Y. Hsub, and X. Jina, “Mobile free space optical communication system,” 2009.
- [23] Y. Yue and Z. Song, “An integral resonant control scheme for a laser beam stabilization system,” in *2015 IEEE International Conference on Information and Automation*, Aug 2015, pp. 2221–2226.
- [24] A. Al-Alwan, X. Guo, I. N’Doye, and T. M. Laleg-Kirati, “Laser beam pointing and stabilization by fractional-order pid control: Tuning rule and experiments,” in *2017 IEEE Conference on Control Technology and Applications (CCTA)*, Aug 2017, pp. 1685–1691.
- [25] B. Potsaid, J. T. yung Wen, M. Unrath, D. Watt, and M. Alpay, “High performance motion tracking control for electronic manufacturing,” *Journal of Dynamic Systems, Measurement, and Control*, pp. 767–776, 2007.

- [26] Y. Shao, D. L. Dickensheets, and P. Himmer, “3-d moems mirror for laser beam pointing and focus control,” *IEEE Journal of Selected Topics in Quantum Electronics*, vol. 10, no. 3, pp. 528–535, May 2004.
- [27] A.Raj, J. A. V. Selvi, and S. Raghavan, “Terrestrial free space line of sight optical communication (tfslsoc) using adaptive control steering system with laser beam tracking, aligning and positioning (atp),” in *2010 International Conference on Wireless Communication and Sensor Computing (ICWCSC)*, Jan 2010, pp. 1–5.
- [28] C. G. T. C. James A., Mynderse, “Modeling of a dynamic mirror with antagonistic piezoelectric stack actuation,” *Journal of Dynamic Systems, Measurement, and Control*, vol. 136, no. 2, pp. 041 001–1, 2013.
- [29] W. Zhu and X. T. Rui, “Modeling of a threedegrees of freedom piezo-actuated mechanism,” *Smart Materials and Structures*, vol. 26, no. 1, p. 015006, 2017.
- [30] H. Chen, A. Chen, W. J. Sun, Z. D. Sun, and J. T. Yeow, “Closed-loop control of a 2-d mems micromirror with sidewall electrodes for a laser scanning microscope system,” *International Journal of Optomechatronics*, vol. 10, no. 1, pp. 1–13, 2016.
- [31] F. Gago, L. Rodriguez-Ramos, G. Herrera, J. Gigante, A. Alonso, T. Viera, J. Piqueras, and J. J. Diaz, “Tip-tilt mirror control based on fpga for an adaptive optics system,” in *2007 3rd Southern Conference on Programmable Logic*, Feb 2007, pp. 19–26.

- [32] Y. F. Liu, J. Li, X. H. Hu, Z. M. Zhang, L. Cheng, Y. Lin, and W. J. Zhang, “Modeling and control of piezoelectric inertiafriction actuators: review and future research directions,” *Mechanical Sciences*, vol. 6, no. 2, pp. 95–107, 2015.
- [33] A. Bergander and J. M. Breguet, “Performance improvements for stick-slip positioners,” in *MHS2003. Proceedings of 2003 International Symposium on Micromechatronics and Human Science (IEEE Cat. No.03TH8717)*, Oct 2003, pp. 59–66.
- [34] J. Y. Peng and X. B. Chen, “Modeling of piezoelectric-driven stickslip actuators,” *IEEE/ASME Transactions on Mechatronics*, vol. 16, no. 2, pp. 394–399, April 2011.
- [35] W. Liu, L. Cheng, C. Zhou, Z. Hou, and M. Tan, “Neural-network based model predictive control for piezoelectric-actuated stick-slip micro-positioning devices,” in *2016 IEEE International Conference on Advanced Intelligent Mechatronics (AIM)*, July 2016, pp. 1312–1317.
- [36] L. Cheng, W. Liu, C. Yang, T. Huang, Z. Hou, and M. Tan, “A neural-network-based controller for piezoelectric-actuated stickslip devices,” *IEEE Transactions on Industrial Electronics*, vol. 65, no. 3, pp. 2598–2607, March 2018.
- [37] M. Rakotondrabe, Y. Haddab, and P. Lutz, “High-stroke motion modelling and voltage/frequency proportional control of a stick-slip microsystem,” in

- Proceedings 2007 IEEE International Conference on Robotics and Automation*, April 2007, pp. 4490–4496.
- [38] Y. Cao and X. Chen, “An arx-based pid-sliding mode control on velocity tracking control of a stick-slip piezoelectric-driven actuator,” *Modern Mechanical Engineering*, vol. 5, no. 01, p. 10, 2015.
- [39] J. Cheng, M. Wu, and L. Chen, “Observer-based tracking control for suppressing stick-slip vibration of drillstring system,” in *2018 37th Chinese Control Conference (CCC)*, July 2018, pp. 10 254–10 258.
- [40] S. Gu and C. Ru, “Design of a novel piezoelectric stick-slip driving nanopositioning stage and power supply circuit,” in *2018 International Conference on Manipulation, Automation and Robotics at Small Scales (MARSS)*, July 2018, pp. 1–4.
- [41] *SmarAct Controller and Software, Versatile Control for Micro and Nano Positioning*, SmatACT.
- [42] *SCU User Manual*, SmatACT.
- [43] *Introduction, Welcome to the world of SmarAct*, SmatACT.
- [44] M. Shao, Z. Wei, M. Hu, and G. Zhang, “Calibration method for a vision guiding-based laser-tracking measurement system,” *Measurement Science and Technology*, vol. 26, no. 8, p. 085009, 2015.

- [45] C. Deng, T. Tang, Y. Mao, and G. Ren, “Enhanced disturbance observer based on acceleration measurement for fast steering mirror systems,” *IEEE Photonics Journal*, vol. 9, no. 3, pp. 1–11, June 2017.
- [46] L. Lou, F. Zhang, Y. Shentu, Y. Si, Y. Zhang, Y. Guo, P. Yang, H. Wang, H. Huang, and H. Song, “Stabilization of laser beam position based on a closed-loop fast steering mirror system,” in *OCEANS 2017 - Aberdeen*, June 2017, pp. 1–6.
- [47] W. Zhao, L. Qiu, Z. Feng, and C. Li, “Laser beam alignment by fast feedback control of both linear and angular drifts,” *Optik - International Journal for Light and Electron Optics*, vol. 117, no. 11, pp. 505 – 510, 2006.
- [48] G. Song, J. Zhao, X. Zhou, and J. A. D. Abreu-Garcia, “Tracking control of a piezoceramic actuator with hysteresis compensation using inverse preisach model,” *IEEE/ASME Transactions on Mechatronics*, vol. 10, no. 2, pp. 198–209, April 2005.
- [49] M. Goldfarb and N. Celanovic, “Modeling piezoelectric stack actuators for control of micromanipulation,” *IEEE Control Systems*, vol. 17, no. 3, pp. 69–79, June 1997.
- [50] G. Wang and F. Bai, “Robust tracking control of piezoelectric fast steering mirror with hysteresis and disturbances correction,” in *2015 34th Chinese Control Conference (CCC)*, July 2015, pp. 389–394.

- [51] T. Sadalla, D. Horla, W. Giernacki, and P. Kozierski, “Stability analysis and tracking performance of fractional-order pi controller for a second-order oscillatory system with time-delay,” in *2016 21st International Conference on Methods and Models in Automation and Robotics (MMAR)*, Aug 2016, pp. 322–326.
- [52] C. A. Monje, Y. Chen, B. M. Vinagre, D. Xue, and V. Feliu-Batlle, *Fractional-order systems and controls: fundamentals and applications*. Springer Science & Business Media, 2010.
- [53] A. Tepljakov, E. Petlenkov, and J. Belikov, “Fomcon: Fractional-order modeling and control toolbox for matlab,” in *Proceedings of the 18th International Conference Mixed Design of Integrated Circuits and Systems - MIXDES 2011*, June 2011, pp. 684–689.
- [54] N. Lachhab, F. Svaricek, F. Wobbe, and H. Rabba, “Fractional order pid controller (fopid)-toolbox,” in *Control Conference (ECC), 2013 European*. IEEE, 2013, pp. 3694–3699.
- [55] R. Malti, M. Aoun, J. Sabatier, and A. Oustaloup, “Tutorial on system identification using fractional differentiation models,” vol. 39, no. 1, pp. 606 – 611, 2006, 14th IFAC Symposium on Identification and System Parameter Estimation.
- [56] A. Narang, *Identification and control of fractional and integer order systems*, 2012, vol. 74, no. 04.

- [57] L. Mingqiu and J. Shuhua, “Design of fo [pi] fractional order controller of atp rough tracking system,” in *2013 Fifth International Conference on Measuring Technology and Mechatronics Automation*, Jan 2013, pp. 442–445.
- [58] R. Porter, B. Shirinzadeh, M. H. Choi, and U. Bhagat, “Sliding mode based laser-beam auto-alignment for laser interferometry-based localisation of multirotor helicopters,” in *2015 IEEE Conference on Control Applications (CCA)*, Sept 2015, pp. 1428–1433.
- [59] A. A. Tseng, “Advancements and challenges in development of atomic force microscopy for nanofabrication,” in *Nano Today*, vol. 6, no. 1, 2011, pp. 4–13.
- [60] G. Binnig and H. Rohrer, “Scanning tunneling microscopy,,” in *Helvetica Phys. Acta*, vol. 55, 1982, pp. 726–735.
- [61] G. Park, M. T. Bement, D. A. Hartman, R. E. Smith, and C. R. Farrar, “The use of active materials for machining processes: A review,” in *Int. J. Machine Tools and Manufacture*, vol. 47, no. 15, 2007, pp. 2189–2206.
- [62] Y. Tian, D. Zhang, and B. Shirinzadeh, “Dynamic modelling of a flexure-based mechanism for ultra-precision grinding operation,” in *Precision Eng*, vol. 35, no. 4, 2011, pp. 554–565.

Vitae

- Name: Syed Ahsan Masud Zaidi
- Nationality: Pakistan
- Date of Birth: 18 – *Oct* – 1990
- Email: *ahsan_zaidi@rocketmail.com*
- Permenant Address: 4-Arya Nagar, Saman Abad Lahore, Pakistan